Contribution from the Department of Chemistry,
University of Hong Kong, Hong Kong

Synthesis, Reactivities, and Structural Studies on High-Valent Ruthenium Oxo Complexes. Ruthenium(IV), Ruthenium(V), and Ruthenium(VI) Oxo Complexes of Tertiary Amine Ligands

Chi-Ming Che,* Ting-Fong Lai,† and Kwok-Yin Wong

Received December 10, 1986

The synthesis and characterization of *trans*-$[Ru^{VI}(L)O_2]^{2+}$, *trans*-$[Ru^{V}(L)O_2]^{+}$, and *trans*-$[Ru^{IV}(L)O(X)]^{n+}$ complexes are described [L = 14-TMC (1,4,8,11-tetramethyl-1,4,8,11-tetraazacyclotetradecane), 15-TMC (1,4,8,12-tetramethyl-1,4,8,12-tetraazapentadecane), 16-TMC (1,5,9,13-tetramethyl-1,5,9,13-tetraazacyclohexadecane), $(TMEA)_2$ (bis(*N,N,N',N'*-tetramethyl-1,2-diaminoethane)); $n = 1$, X = Cl, N_3, NCO; $n = 2$, X = CH_3CN]. All *trans*-Ru(VI)–dioxo complexes are diamagnetic whereas the molar magnetic susceptibilities for *trans*-$[Ru^{V}(L)O_2]^{+}$ and *trans*-$[Ru^{IV}(L)O(X)]^{n+}$ systems are 1.94 and 2.70–2.95 μ_B, respectively. In CH_3CN, *trans*-$[Ru^{VI}(L)O_2]^{2+}$ and *trans*-$[Ru^{V}(L)O_2]^{+}$ exhibit vibronic-structured $d_{xy} \rightarrow d_{\pi}^*$ ($d_{\pi}^* = d_{xz}$, d_{yz}) transition bands centered at ~380 and 430 nm, respectively. The X-ray structure of *trans*-$[Ru^{IV}$(14-TMC)O(NCO)$]ClO_4$ has been determined: $C_{15}H_{32}N_5O_2RuClO_4$, M_r 514.97, orthorhombic, space group *Pnma*, a = 12.507 (2) Å, b = 10.646 (1) Å, c = 15.681 (2) Å, V = 2088.1 Å^3, $Z = 4$, d_{calcd} = 1.638 g cm^{-3}, μ(Mo Kα) = 9.14 cm^{-1}, m = 1943. The Ru=O bond distances of *trans*-$[Ru^{IV}$(14-TMC)O(X)$]^{n+}$ are all 1.765 Å, which are longer than those for *trans*-$[Ru^{VI}(L)O_2]^{2+}$ (1.70–1.71 Å). The $E_{1/2}$ value for the *trans*-$[Ru^{V}(L)O(X)]^{2+}$/*trans*-$[Ru^{IV}(L)O(X)]^{+}$ couple lies between 0.70 and 1.10 V vs. the $Cp_2Fe^{+/0}$ couple and decreases in the order X = Cl > NCO > N_3. All *trans*-$[Ru^{IV}(L)O(X)]^{n+}$ complexes are active electrocatalysts for the oxidation of benzyl alcohol to benzaldehyde. The $E_{1/2}$ values for the *trans*-$[Ru^{VI}(L)O_2]^{2+}$/*trans*-$[Ru^{IV}(L)O(OH_2)]^{2+}$ and *trans*-$[Ru^{VI}(L)O_2]^{2+}$/*trans*-$[Ru^{V}(L)O_2]^{+}$ couples are insensitive to the macrocyclic hole size of L. Replacement of the σ-saturated tertiary amine by the π-aromatic pyridine or 2,2'-bipyridine weakens the Ru=O bond and increases the oxidation potential of the Ru=O complexes. Studies on the reactions of *trans*-$[Ru^{VI}(L)O_2]^{2+}$ and *trans*-$[Ru^{VI}(TMP)O_2]$ (H_2TMP = 5,10,15,20-tetramesitylporphyrin) with organic substrates indicated that the former system prefers attack on an activated C–H bond.

Introduction

High-valent oxo complexes of ruthenium have long been known to be active oxidants in the oxidation of organic substrates.[1] "RuO_4", though a powerful oxidizing agent, is severely limited in its application in organic synthetic reactions because its reactions are usually nonspecific. Other known "Ru^{IV}=O" complexes, such as $RuO_2 \cdot xH_2O$, have poorly understood oxidation chemistry although they find useful applications in photochemical water splitting and the electrochemical chloride oxidation reaction.[2] Meyer and co-workers first underlined the importance of studying the chemistry and reactivity of "Ru=O" complexes containing nonlabile oxidation-resistant ligands.[3] Their extensive works on $[Ru^{IV}(trpy)(bpy)O]^{2+}$ (trpy = 2,2':6',2''-terpyridine; bpy = 2,2'-bipyridine) and related complexes have aroused our interest in this area.[3] However, ruthenium oxo complexes containing π-aromatic amines are difficult to study owing to their instabilities and low solubilities in aqueous medium. Macrocyclic tertiary amines, such as 14-TMC (1,4,8,11-tetramethyl-1,4,8,11-tetraazacyclotetradecane) (Figure 1) have long been known to encapsulate transition-metal ions in unusual oxidation states. For example, stable low-valent Ni(I) and Cu(I) complexes[4,5] of the saturated tetraazamacrocyclic ligand 1,4,5,7,7,8,11,12,14,14-decamethyl-1,4,8,11-tetraazacyclotetradecane could be generated in aqueous solution. The tertiary amine ligands 14-TMC, 15-TMC (1,4,8,12-tetramethyl-1,4,8,12-tetraazacyclopentadecane) and 16-TMC (1,5,9,13-tetramethyl-1,5,9,13-tetraazacyclohexadecane) (Figure 1)[6,7] are attractive to us because they are resistant toward oxidation upon complexation to a metal ion. Furthermore, charge-transfer mixing of the amine with the Ru=O bond is reduced to a minimum because of its pure σ-saturated nature. Spectroscopic studies on the "Ru=O" unit with the metal ion in different oxidation states are thus feasible with these ligands. In this contribution, we present a detailed picture on the chemistry and reactivities of "Ru=O" complexes with the central metal ion in oxidation state of +4, +5, or +6; part of the work described in this context has previously been communicated.[8]

Experimental Section

The tertiary amine ligands 14-TMC, 15-TMC, and 16-TMC were prepared as previously described.[6,7] $K_2[RuCl_5(H_2O)]$ was obtained from Johnson Matthey Chemicals, Ltd. Tetrabutylammonium perchlorate ($[Bu_4N]ClO_4$, Southwestern Analytical Chemicals, electrometric grade) was dried in vacuum at 60 °C for 48 h before use. Acetonitrile (Mallinckrodt chromAR) was twice distilled over CaH_2 under argon. All other solvents and chemicals in synthetic work were analytical grade and used without further purification. *trans*-$[Ru^{III}(L)Cl_2]Cl$[6,9] (L = 14-TMC, 15-TMC, 16-TMC, $(TMEA)_2$ (TMEA = *N,N,N',N'*-tetramethyl-1,2-diaminoethane)), *trans*-$[Ru^{VI}$(14-TMC)$O_2][ClO_4]_2$,[10] and *trans*-$[Ru^{VI}(TMP)O_2]$ (H_2TMP = 5,10,15,20-tetramesitylporphyrin)[11]

* To whom correspondence should be addressed.

† X-ray structural data for *trans*-$[Ru^{IV}$(14-TMC)O(NCO)$]ClO_4$ were collected at Caltech by T.-F.L. during her leave from the University of Hong Kong.

(1) (a) Courtney, J. L.; Swanborough, K. F. *Rev. Pure Appl. Chem.* **1972**, *47*, 22. (b) Lee, D. G.; Vanden Engh, M. *Org. Chem. (N.Y.)* **1973**, *58*, 177. (c) Seddon, E. A.; Seddon, K. R. In *The Chemistry of Ruthenium*; Elsevier: Amsterdam, 1984; p 57. (d) Meyer, T. J. *J. Electrochem. Soc.* **1984**, *131*, 221c. (e) Torii, S.; Inokuchi, T.; Sugiura, T. *J. Org. Chem.* **1986**, *51*, 155. (f) Carlsen, P. H. J.; Katsuki, T.; Martin, V. S.; Sharpless, K. B. *J. Org. Chem.* **1981**, *46*, 3936.

(2) (a) Borgarello, E.; Kiwi, J.; Pelizzetti, F.; Visca, M.; Gratzel, M. *J. Am. Chem. Soc.* **1981**, *103*, 6324. (b) Ellis, C. D.; Gilbert, J. A.; Murphy, W. R., Jr.; Meyer, T. J. *J. Am. Chem. Soc.* **1983**, *105*, 4842.

(3) (a) Moyer, B. A.; Meyer, T. J. *Inorg. Chem.* **1981**, *20*, 436. (b) Takeuchi, K. J.; Thompson, M. S.; Pipes, D. W.; Meyer, T. J. *Inorg. Chem.* **1984**, *23*, 1845. (c) Moyer, B. A.; Thompson, M. S.; Meyer, T. J. *J. Am. Chem. Soc.* **1980**, *102*, 2310. (d) Thompson, M. S.; Meyer, T. J. *J. Am. Chem. Soc.* **1982**, *104*, 4106, 5070. (e) Samuels, G. J.; Meyer, T. J. *J. Am. Chem. Soc.* **1981**, *103*, 307. (f) Moyer, B. A.; Meyer, T. J. *J. Am. Chem. Soc.* **1978**, *100*, 3601. (g) Gilbert, J. A.; Eggleston, D. S.; Murphy, W. R., Jr.; Geselowitz, D. A.; Gersten, G. W.; Hodgson, D. J.; Meyer, T. J. *J. Am. Chem. Soc.* **1985**, *107*, 3855. (h) Thompson, M. S.; DeGiovani, W. F.; Moyer, B. A.; Meyer, T. J. *J. Org. Chem.* **1984**, *49*, 4972.

(4) (a) Jubran, N.; Ginzburg, G.; Cohen, H.; Koresh, Y.; Meyerstein, D. *Inorg. Chem.* **1985**, *24*, 251. (b) Jubran, N.; Cohen, H.; Meyerstein, D. *J. Chem. Soc., Chem. Commun.* **1982**, 517.

(5) Jubran, N.; Cohen, H.; Koresh, Y.; Meyerstein, D. *J. Chem. Soc., Chem. Commun.* **1984**, 1683.

(6) Che, C. M.; Wong, K. Y.; Poon, C. K. *Inorg. Chem.* **1986**, *25*, 1809.

(7) (a) Alcock, N. W.; Curzon, E. H.; Moore, P.; Pierpoint, C. *J. Chem. Soc., Dalton Trans* **1984**, 605. (b) Barefield, E. K.; Wagner, F. *Inorg. Chem.* **1973**, *12*, 2435.

(8) (a) Che, C. M.; Wong, K. Y.; Mak, T. C. W. *J. Chem. Soc., Chem. Commun.* **1985**, 546. (b) Che, C. M.; Wong, K. Y.; Mak, T. C. W. *Ibid.* **1985**, 988. (c) Mak, T. C. W.; Che, C. M.; Wong, K. Y. *Ibid.* **1985**, 986. (d) Che, C. M.; Wong, K. Y. *Ibid.* **1986**, 229.

(9) Che, C. M.; Kwong, S. S.; Poon, C. K. *Inorg. Chem.* **1985**, *24*, 1601.

(10) Che, C. M.; Wong, K. Y.; Poon, C. K. *Inorg. Chem.* **1985**, *24*, 1797.

0020-1669/87/1326-2289$01.50/0

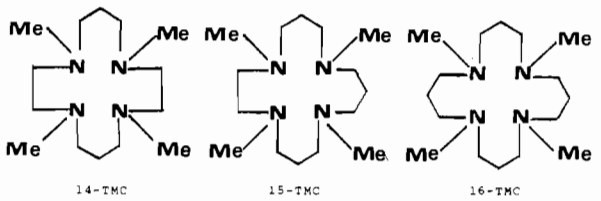

Figure 1. Structures of macrocyclic tertiary amines.

were prepared by literature methods.

***trans*-[Ru^{VI}(15-TMC)O$_2$][Y]$_2$ (Y = ClO$_4$, PF$_6$).** *trans*-[Ru^{III}(15-TMC)Cl$_2$]Cl (0.3 g) and silver toluene-*p*-sulfonate (0.54 g) in H_2O (25 mL) were heated to about 60 °C for $^1/_2$ h. The resulting yellow solution (sometimes brownish yellow) was filtered to remove the insoluble AgCl. Hydrogen peroxide (30%, 3 mL) was slowly added into the filtrate while the solution was kept at 60 °C for 5 min. The solution was then cooled in an ice bath. Upon addition of a saturated solution of $NaClO_4$, yellow microcrystalline solid *trans*-[Ru^{VI}(15-TMC)O$_2$][ClO$_4$]$_2$ slowly deposited, which was filtered and recrystallized from hot $HClO_4$ (0.1 M, 60 °C). The hexafluorophosphate salt was similarly prepared by using $[NH_4]PF_6$ instead of $NaClO_4$ (yield ~50%). Anal. Calcd for [Ru^{VI}(15-TMC)O$_2$][ClO$_4$]$_2$: C, 29.2; H, 5.7; N, 9.3; Cl, 11.7. Found: C, 29.6; H, 5.8; N, 9.4; Cl, 11.5.

***trans*-[Ru^{VI}(TMEA)O$_2$][ClO$_4$]$_2$.** This was similarly prepared as described for *trans*-[Ru^{VI}(15-TMC)O$_2$][ClO$_4$]$_2$ with *trans*-[Ru^{III}(TMEA)$_2$Cl$_2$]Cl as the starting material. Yield: ~23%. Anal. Calcd for [Ru^{VI}(TMEA)$_2$O$_2$][ClO$_4$]$_2$: C, 25.5; H, 5.7; N, 9.9; Cl, 12.5. Found: C, 25.5; H, 6.0; N, 10.1; Cl, 12.2.

***trans*-[Ru^{VI}(16-TMC)O$_2$][ClO$_4$]$_2$.** *trans*-[Ru^{III}(16-TMC)Cl$_2$]Cl (0.3 g) and silver toluene-*p*-sulfonate (0.7 g) in water (25 ml) were heated at boiling for $1^1/_2$ h. The hot solution was filtered to remove the insoluble AgCl. Hydrogen peroxide (30%, 3 mL) was slowly added to the filtrate that was kept at 60 °C for 5 min. This was then ice-cooled. Upon addition of a saturated solution of $NaClO_4$, yellow solid *trans*-[Ru^{VI}(16-TMC)O$_2$][ClO$_4$]$_2$ slowly deposited. The crude solid was recrystallized in hot $HClO_4$ (0.1 M, 60 °C). The yield was 23%. Anal. Calcd for [Ru^{VI}(16-TMC)O$_2$][ClO$_4$]$_2$: C, 31.2; H, 5.8; N, 9.1; Cl, 11.5. Found: C, 31.2; H, 5.8; N, 9.1; Cl, 11.4.

***trans*-[Ru^{IV}(14-TMC)O(CH$_3$CN)][PF$_6$]$_2$.** *trans*-[Ru^{VI}(14-TMC)O$_2$](PF$_6$)$_2$ (0.5 g) and PPh_3 (0.7 g) were stirred in acetone–acetonitrile mixture (1:1 v/v, 20 mL) for 1 h. Bright yellow crystals of *trans*-[Ru^{IV}(14-TMC)O(CH$_3$CN)(PF$_6$)$_2$ slowly deposited upon standing. This was further recrystallized by slow diffusion of diethyl ether into an acetonitrile solution of the crude solid (yield ~25%). Anal. Calcd for [Ru^{IV}(14-TMC)O(CH$_3$CN)][PF$_6$]$_2$: C, 27.3; H, 5.0; N, 9.9; P, 8.8. Found: C, 27.0; H, 5.0; N, 9.9; P, 9.2.

***trans*-[Ru^{IV}(15-TMC)O(CH$_3$CN)][ClO$_4$]$_2$.** This was similarly prepared as described for *trans*-[Ru^{IV}(14-TMC)O(CH$_3$CN)][PF$_6$]$_2$. Anal. Calcd for [Ru^{IV}(15-TMC)O(CH$_3$CN)][ClO$_4$]$_2$: C, 32.5; H, 5.9; N, 11.2; Cl, 11.3. Found: C, 32.7; H, 5.9; N, 11.2; Cl, 11.7.

***trans*-[Ru^{IV}(14-TMC)O(Cl)]ClO$_4$.** *trans*-[Ru^{VI}(14-TMC)O$_2$][ClO$_4$]$_2$ (0.5 g) and PPh_3 (3 g) were stirred in acetone (~30 mL) at room temperature for 1 h. A deep yellow solution was obtained. Upon addition of diethyl ether, yellow solid *trans*-[Ru^{IV}(14-TMC)O(Cl)]ClO$_4$ was precipitated off, which was recrystallized by slow diffusion of diethyl ether into an acetone solution of the crude product (~80%). Anal. Calcd. for [Ru^{IV}(14-TMC)O(Cl)]ClO$_4$: C, 33.1; H, 6.3; N, 11.0; Cl, 14.0. Found: C, 33.5; H, 6.6; N, 11.4; Cl, 14.0.

***trans*-[Ru^{IV}(15-TMC)O(Cl)]ClO$_4$.** This was similarly prepared from *trans*-[Ru^{VI}(15-TMC)O$_2$][ClO$_4$]$_2$. Anal. Calcd for [Ru^{IV}(15-TMC)O(Cl)]ClO$_4$: C, 34.5; H, 6.5; N, 10.7; Cl, 13.5. Found: C, 34.8; H, 7.0; N, 10.8; Cl, 13.3.

***trans*-[Ru^{IV}(TMEA)$_2$O(Cl)]ClO$_4$.** This was similarly prepared from *trans*-[Ru^{VI}(TMEA)$_2$O$_2$][ClO$_4$]$_2$. Anal. Calcd for [Ru^{IV}(TMEA)$_2$O(Cl)]ClO$_4$: C, 29.8; H, 6.6; N, 11.6; Cl, 14.6. Found: C, 29.8; H, 6.6; N, 11.7; Cl, 14.4.

***trans*-[Ru^{IV}(14-TMC)O(NCO)]ClO$_4$.** *trans*-[Ru^{III}(14-TMC)Cl$_2$]Cl (0.3 g) and silver toluene-*p*-sulfonate (0.6 g) in deionized water (25 mL) were heated to about 60 °C for $^1/_2$ h. The insoluble AgCl was filtered off, and the filtrate was warmed to about 60 °C on a steam bath. NaNCO (0.1 g) was added to the solution followed by the immediate addition of H_2O_2 (30%, 1 mL). The solution was swirled until effervescence ceased. Additional NaNCO (0.5 g) was added in, and the resulting brown solution was filtered off to remove any insoluble materials. Upon addition of solid $NaClO_4$ to the filtrate and cooling, golden brown needle-shaped crystals of *trans*-[Ru^{IV}(14-TMC)O(NCO)]ClO$_4$ slowly deposited (yield ~24%). Anal. Calcd for [Ru^{IV}(14-TMC)O(NCO)]ClO$_4$: C, 35.0; H, 6.2; N, 13.6; Cl, 6.9. Found: C, 34.8; H, 6.5; N, 13.6; Cl, 7.1.

***trans*-[Ru^{IV}(14-TMC)O(N$_3$)]ClO$_4$.** *trans*-[Ru^{III}(14-TMC)Cl$_2$]Cl (0.3 g) and silver toluene-*p*-sulfonate (0.6 g) in deionized water (25 mL) were heated to about 60 °C for $^1/_2$ h. The solution was filtered to remove the insoluble AgCl. The filtrate was warmed to about 60 °C on a steam bath. NaN_3 (0.1 g) was added to the solution followed by the addition of H_2O_2 (30 mL). The solution was swirled until effervescence ceased. Additional NaN_3 (0.5 g) was then added in. A brown solution was obtained and filtered to remove any insoluble materials. Upon addition of solid $NaClO_4$ to the filtrate and cooling, brown needle-shaped crystals of *trans*-[Ru^{IV}(14-TMC)O(N$_3$)]ClO$_4$ slowly deposited (yield ~38%). Anal. Calcd for [Ru^{IV}(14-TMC)O(N$_3$)]ClO$_4$: C, 32.6; H, 6.2; N, 19.0; Cl, 6.9. Found: C, 32.6; H, 6.3; N, 19.2; Cl, 7.1.

***trans*-[Ru^{IV}(15-TMC)O(N$_3$)]ClO$_4$.** This was similarly prepared as described for *trans*-[Ru^{IV}(14-TMC)O(N$_3$)]ClO$_4$. Anal. Calcd for [Ru^{IV}(15-TMC)O(N$_3$)]ClO$_4$: C, 34.0; H, 6.4; N, 18.5; Cl, 6.7. Found: C, 33.6; H, 6.3; N, 18.3; Cl, 6.9.

***trans*-[Ru^{V}(14-TMC)O$_2$]ClO$_4$.** Preparation of this compound was carried out in a dry-atmosphere glovebox. *Trans*-[Ru^{VI}(14-TMC)O$_2$][ClO$_4$]$_2$ (0.1 g) in an acetonitrile solution of [Bu$_4$N]ClO$_4$ (0.1 M) was electrolyzed at constant potential [–0.3 V vs. Ag/AgNO$_3$ (0.1 M in CH_3CN)] under argon atmosphere by using a glassy-carbon cup as the working electrode. The solution was stirred to ensure rapid electrolysis. When the current flow had ceased, anhydrous diethyl ether was added to the solution. The precipitated yellow solid of *trans*-[Ru^{V}(14-TMC)O$_2$]ClO$_4$ was filtered and washed with anhydrous diethyl ether (yield ~80%). The solid was found to be very hygroscopic. Anal. for [Ru^{V}(14-TMC)O$_2$]ClO$_4$: C, 34.4; H, 6.6; N, 11.5; Cl, 7.3. Found: C, 34.0; H, 7.0; N, 11.0; Cl, 7.7.

***trans*-[Ru^{V}(L)O$_2$]ClO$_4$ (L = 15-TMC, 16-TMC, (TMEA)$_2$).** Acetonitrile solutions of *trans*-[Ru^{V}(15-TMC)O$_2$]$^+$, *trans*-[Ru^{V}(16-TMC)O$_2$]$^+$, and *trans*-[Ru^{V}(TMEA)$_2$O$_2$]$^+$ were similarly prepared by constant-potential electrolytic reduction of the corresponding *trans*-dioxoruthenium(VI) complexes. No attempts were made to isolate these compounds out as solids. Except for *trans*-[Ru^{V}(TMEA)$_2$O$_2$]$^+$, these solutions were fairly stable even upon prolonged storage (more than 1 week in a ground glass joint stoppered flask at 0 °C).

Physical Measurements and Instrumentation. UV–vis spectra were obtained on a Beckman Acta III spectrophotometer. Infrared spectra were obtained as Nujol mulls on a Perkin-Elmer Model 577 spectrophotometer (4000–200 cm^{-1}). Mass spectra were run by using a Hitachi Model RMS-4 single-focusing magnetic sector mass spectrometer. Magnetic susceptibilities were measured by using the Guoy method with mercury tetrakis(thiocyanato)cobaltate(II) as calibrant. Conductivity measurements were performed with a Radiometer Model CDM2 conductivity meter with 0.1 M KCl as calibrant. Constant-potential electrolyses were performed by using a Princeton Applied Research Model 173 potentiostat with a Model 337A coulometric cell system. Elemental analyses of the new complexes were performed by the Microanalytical Unit of the Australian Mineral Development. The formal potentials of the ruthenium complexes were measured by cyclic voltammeric techniques using a Princeton Applied Research (PAR) Model 175 universal programmer, Model 173 potentiostat, and Model 179 digital coulometer.

Gas Chromatographic Analysis of the Organic Products in the Oxidation Reactions of Ruthenium Oxo Complexes. The organic reactants, benzyl alcohol, cyclohexanone, and cyclohexanol were purified by fractional distillation under vacuum and their purities were checked by gas chromatography (GC). No impurity peaks were observed with a flame ionization detector of 10^{-11} A/mV sensitivity. Cyclohexene, cyclohexane, and toluene were distilled under argon, and their purities were also checked by GC. Reactions between the ruthenium oxo complexes and various organic substrates were performed either by dissolving both reactants in a solvent or by suspending the ruthenium complex (50–100 mg) in the liquid substrate (1 mL). The reaction mixture was stirred with a magnet bar, and the temperature was maintained at ±1 °C by a thermostated water bath. A control experiment in the absence of the ruthenium complexes was performed for each reaction. The organic products were analyzed by GC and IR, NMR, and UV–vis spectroscopy. Gas chromatographic analyses were conducted by using a Varian 2440 gas chromatograph with flame ionization detector. A 10% w/w Carbowax 20M on Chromosorb W (80–100 mesh size) $^1/_8$ in. × 6 ft stainless-steel column was used with nitrogen or helium as the carrier gas. Component identification was established by comparing the retention time with an authentic sample as well as by gas chromatographic mass spectral analysis. Quantitation of individual gas chromatographic components was done by the internal standard method employing a Hewlett-Packard 3380A electronic integrator. Benzyl acetate and *n*-decyl alcohol were used as internal standards in the quantitative analyses

(11) Groves, J. T.; Quinn, R. *Inorg. Chem.* **1984**, *23*, 3844.

Table I

Fractional Coordinates[a] and Thermal Parameters[b]

atom	x	y	z	U_{eq} or U
Ru	18113 (4)	25000	13068 (3)	367 (1)[c]
N(1)	1337 (4)	1027 (5)	2147 (3)	54 (1)[c]
N(2)	2191 (4)	1013 (5)	446 (3)	60 (1)[c]
C(1)	985 (9)	21 (12)	1545 (7)	76 (3)
C(1′)	1856 (13)	−27 (18)	1884 (10)	59 (5)
C(2)	1740 (6)	−170 (7)	861 (5)	85 (2)[c]
C(3)	1686 (5)	1276 (9)	−388 (4)	85 (2)[c]
C(4)	2009 (9)	2500	−803 (6)	101 (5)[c]
C(5)	887 (8)	2500	3342 (6)	82 (3)[c]
C(6)	591 (9)	1333 (11)	2753 (6)	71 (4)
C(6′)	1538 (13)	1473 (17)	3024 (10)	57 (5)
C(7)	3378 (5)	798 (8)	313 (5)	84 (2)[c]
C(8)	2333 (8)	435 (10)	2626 (6)	70 (3)
C(8′)	69 (14)	738 (17)	2204 (10)	57 (5)
N(3)	220 (5)	2500	843 (4)	53 (2)[c]
C(9)	−697 (6)	2500	766 (5)	46 (2)[c]
O(1)	−1645 (4)	2500	665 (4)	74 (2)[c]
O(2)	3121 (4)	2500	1726 (3)	52 (1)[c]
Clk	450 (2)	2500	6624 (2)	71 (1)[c]
O(3)	1515 (18)	2500	6815 (14)	158 (10)
O(3′)	78 (18)	2500	7532 (15)	106 (10)
O(4)	−657 (17)	2500	6865 (13)	147 (10)
O(4′)	734 (27)	2500	5724 (23)	211 (11)
O(5)	171 (10)	1422 (13)	6220 (7)	145 (5)
O(5′)	970 (20)	1563 (20)	7130 (14)	134 (10)

Occupancy Factors for Partial Atoms

atom	occupancy factor	atom	occupancy factor
C(1), C(6), C(8)	0.64 (1)	C(1′), C(6′), C(8′)	0.36 (1)
O(3)	0.59 (2)	O(3′)	0.41 (2)
O(4)	0.54 (2)	O(4′)	0.46 (2)
O(5)	0.67 (1)	O(5′)	0.33 (1)

[a] $\times 10^5$ for Ru; $\times 10^4$ for other atoms. [b] Å$^2 \times 10^4$ for Ru; Å$^2 \times 10^3$ for other atoms. [c] Equivalent isotrtopic thermal parameter: $U_{eq} = {}^1/_3\sum_i\sum_j U_{ij}a^*_i a^*_j \mathbf{a}_i \cdot \mathbf{a}_j$. The exponent of the isotropic thermal parameter takes the form $-8\pi^2 U(\sin^2\theta)/\lambda^2$.

benzaldehyde and 2-cyclohexen-1-one respectively.

X-ray Structural Determination. The crystal structures of *trans*-$[Ru^{VI}(15\text{-TMC})O_2][ClO_4]_2$, *trans*-$[Ru^{VI}(16\text{-TMC})O_2][ClO_4]_2$, *trans*-$[Ru^{IV}(14\text{-TMC})O(CH_3CN)][PF_6]_2$, and *trans*-$[Ru^{IV}(14\text{-TMC})O(Cl)][ClO_4]$ have previously been communicated.[8] For simplicity, only the selected bond distances and angles of these four compounds are included in the text here. *trans*-$[Ru^{IV}(14\text{-TMC})O(NCO)]ClO_4$ has been characterized by X-ray crystallography.

Crystal Data. $C_{15}H_{32}N_5O_2Ru\cdot ClO_4$, M_r 514.97, orthorhombic, space group *Pnma*, a = 12.507 (2) Å, b = 10.646 (1) Å, c = 15.681 (2) Å, V = 2088.1 Å^3, Z = 4, d_{calcd} = 1.638 g cm^{-3}, μ(Mo Kα) = 9.14 cm^{-1}.

Intensity data were collected from a crystal of approximately 0.12 × 0.15 × 0.18 mm on a Nonius CAD4 diffractometer by using the ω–2θ scanning technique in the bisecting mode. Reflections within the $h,k,\pm l$ quadrants extending to $2\theta_{max}$ = 50 were measured. A total of 1943 unique reflections were obtained of which 1811 had net intensity (I) greater than zero. Three check reflections monitored continuously throughout the data collections gave no indication of intensity loss. No absorption correction was applied.

Structural Determination and Refinement. The structure was solved by Patterson and Fourier methods and refined by full-matrix least squares. The quantity minimized was $\sum w(F_o^2 - F_c^2)^2$, with weight $w = 1/\sigma^2(F_o^2)$. Atomic scattering factors were taken from ref 12 with an anomalous dispersion correction applied to those of ruthenium and chlorine.

During the early stage of refinement carbon atoms C(1), C(6), and C(8) in the macrocycle and the oxygen atoms in the perchlorate ion showed abnormally large thermal motion; each of these atoms was subsequently refined isotropically over two sites with initial site occupancy factors of 0.5. All the methylene hydrogen atoms were kept at calculated positions with assigned isotropic thermal factors, but contribution from the methyl hydrogen atoms was omitted. In the final cycles of refinement all non-hydrogen atoms except the partial atoms were refined with anisotropic thermal parameters. In the final cycles of refinement all non-hydrogen atoms except the partial atoms were refined with anisotropic thermal parameters. The final R value $[=\sum||F_o| - |F_c||/\sum|F_o|]$ is 0.051 for 1811 reflections with $F_o^2 > 0$ and 0.047 for 1652 reflections with $F_o^2 > 3\sigma(F_o^2)$. The goodness of fit $[=\sum w(F_o^2 - F_c^2)^2/(m-p)]$ is 4.10 for 1943 measurements (m) and 142 paramaters (p). An attempt has been tried to refine the structure in $Pna2_1$. However, the structure could not be refined to a stage where reasonable bond distances and angles and a satisfactory R factor could be obtained. In view of this, the space group assignment of *Pnma* is prefered.

The atomic coordinates and thermal parameters are listed in Table I. Selected bond distances and angles are tabulated in Table II. Anisotropic thermal parameters and tables of calculated and observed structure factors are available as supplementary material.

Table II. Bond Distances and Angles in $[Ru^{IV}(14\text{-TMC})(NCO)O]ClO_4$

(a) Distances (Å)

Ru–N(1)	2.132 (5)	C(1)–C(2)	1.443 (14)
Ru–N(2)	2.134 (5)	C(1′)–C(2)	1.618 (18)
Ru–N(3)	2.119 (6)	C(2)–N(2)	1.525 (9)
Ru–O(2)	1.765 (5)	N(2)–C(3)	1.479 (9)
N(1)–C(1)	1.493 (12)	N(2)–C(7)	1.517 (9)
N(1)–C(1′)	1.360 (17)	C(3)–C(4)	1.512 (12)
N(1)–C(6)	1.372 (12)	C(5)–C(6)	1.592 (14)
N(1)–C(6′)	1.477 (12)	C(5)–C(6′)	1.452 (19)
N(1)–C(8)	1.585 (12)	N(3)–C(9)	1.154 (10)
N(1)–C(8′)	1.618 (17)	C(9)–O(1)	1.196 (10)

(b) Angles (deg)

N(1)–Ru–O(2)	91.6 (2)	C(8′)–N(1)–C(6′)	100.1 (9)
N(2)–Ru–O(2)	91.7 (2)	C(2)–N(2)–Ru	105.1 (4)
N(3)–Ru–O(2)	178.7 (2)	C(3)–N(2)–Ru	108.9 (4)
N(1)–Ru–N(1)[a]	94.6 (2)	C(7)–N(2)–Ru	114.6 (4)
N(2)–Ru–N(1)	84.6 (2)	C(3)–N(2)–C(2)	112.0 (5)
N(3)–Ru–N(1)	87.2 (2)	C(7)–N(2)–C(2)	107.3 (5)
N(2)–Ru–N(2)[a]	85.9 (2)	C(7)–N(2)–C(3)	109.0 (5)
N(3)–Ru–N(2)	89.5 (2)	C(9)–N(3)–Ru	165.9 (6)
C(1)–N(1)–Ru	102.6 (5)	C(2)–C(1)–N(1)	112.2 (8)
C(1′)–N(1)–Ru	106.7 (8)	C(2)–C(1′)–N(1)	109.6 (11)
C(6)–N(1)–Ru	116.2 (5)	C(1)–C(2)–N(2)	116.2 (7)
C(6′)–N(1)–Ru	107.0 (7)	C(1′)–C(2)–N(2)	108.1 (8)
C(8)–N(1)–Ru	111.5 (5)	C(4)–C(3)–N(2)	115.5 (6)
C(8′)–N(1)–Ru	116.5 (6)	C(3)–C(4)–C(3)[a]	119.0 (8)
C(6)–N(1)–C(1)	114.1 (7)	C(6)–C(5)–C(6)[a]	102.5 (8)
C(8)–N(1)–C(1)	104.2 (6)	C(6′)–C(5)–C(6′)[a]	97.8 (12)
C(6′)–N(1)–C(1′)	117.8 (10)	C(5)–C(6)–N(1)	115.5 (8)
C(8′)–N(1)–C(1′)	109.1 (10)	C(5)–C(6′)–N(1)	117.9 (12)
C(8)–N(1)–C(6)	107.5 (7)	N(3)–C(9)–O(1)	178.6 (8)

[a] Symmetry code: x, ${}^1/_2 - y$, z.

Results and Discussion

The general synthetic routes for *trans*-dioxoruthenium(VI) complexes are outlined as follows:

$$RuO_4 + 4NH_4Cl \xrightarrow{H_2O} trans\text{-}[Ru^{VI}(NH_3)_4O_2]^{2+}\ ^{14} \quad (I)$$

$$trans\text{-}[Ru^{III}(bpy)_2(OH)(OH_2)]^{2+} + Ce(IV) \xrightarrow{ClO_4^-} trans\text{-}[Ru^{VI}(bpy)_2O_2][ClO_4]_2\ ^{15} \quad (II)$$

$$trans\text{-}[Ru^{III}(L)(OH_2)_2]^{3+} + H_2O_2 \rightarrow trans\text{-}[Ru^{VI}(L)O_2]^{2+}\ ^{8} \quad (III)$$

L = 14-TMC, 15-TMC, 16-TMC, $(TMEA)_2$

$$[Ru^{II}(TMP)(CO)] + RC(=O)OOH \rightarrow trans\text{-}[Ru^{VI}(TMP)O_2]^{11} \quad (IV)$$

Route I was developed by Griffith and co-workers.[14] Other complexes like *trans*-$[Ru^{VI}(C_2O_4)_2O_2]^{2-}$ and *trans*-$[Ru^{VI}(X)_4O_2]^{2-}$ (X = Cl, Br) were also prepared in this way. However, insertion of RuO_4 into the macrocyclic amine is not feasible owing to its

(12) *International Tables for X-ray Crystallography*; Kynoch: Birmingham, England, 1974; Vol. 4, p 72.
(13) CRYM system of crystallographic programs developed by R. E. Marsh and co-workers at the California Institute of Technology, 1984.
(14) Griffith, W. P.; Pawson, D. *J. Chem. Soc., Dalton Trans.* **1973**, 1315.
(15) Che, C. M.; Wong, K. Y.; Leung, W. H.; Poon, C. K. *Inorg. Chem.* **1986**, *25*, 345.

instability. Recent works by Groves and co-workers showed that high-valent dioxo(porphyinato)ruthenium(VI) complexes could be obtained by oxidation of $[Ru^{II}P(CO)]$ (P = porphyinate dianion) with organic peracid.[11] The oxidation of Ru(II) and Ru(III) complexes (routes II–IV) *containing labile axial ligands by chemical oxidizing agents like* H_2O_2, Ce(IV), or RC(=O)OOH appears to be the general synthetic methodology for *trans*-dioxoruthenium(VI) systems containing neutral nonlabile amine ligands.

Meyer and co-workers[3c] showed that oxidation of a *single* Ru^{II}—OH_2 *unit* in complexes *containing nonlabile oxidation resistant ligands led to a* Ru^{IV}=O *compound.* Thus $[Ru^{IV}(trpy)(bpy)O]^{2+}$ was obtained by Br_2 oxidation of $[Ru^{II}(trpy)(bpy)(OH_2)]^{2+}$.[3c] However, the applicability of this procedure to other Ru^{IV}=O complexes is quite limited due to the difficulties involved in the preparation of the Ru^{II}—OH_2 precursor. Two other methods have been developed for *trans*-$[Ru^{IV}(L)O(X)]^{n+}$ systems (n = 1, X = Cl, NCO, N_3; n = 2, X = CH_3CN). The first method is the PPh_3 reduction of *trans*-$[Ru^{VI}(L)O_2]^{2+}$.

$$trans\text{-}[Ru^{VI}(L)O_2]^{2+} + PPh_3 + X \xrightarrow{k_1} trans\text{-}[Ru^{IV}(L)O(X)]^{n+} \quad (1)$$

$$trans\text{-}[Ru^{IV}(L)O(X)]^{n+} + PPh_3 \xrightarrow{k_2} [Ru(II)] + O{=}PPh_3 \quad (2)$$

Reactions 1 and 2 are concerted oxo transfer reactions, as PPh_3 is known to be an oxygen atom acceptor: Isolation of Ru^{IV}=O complexes is feasible only if $k_1 \gg k_2$. This is the case for the *trans*-$[Ru^{VI}(L)O_2]^{2+}$ system. Preliminary kinetic measurements[16] on *trans*-$[Ru^{VI}(14\text{-TMC})O_2]^{2+}$ revealed a bimolecular rate law, rate = k[Ru(VI)][PPh_3] with $k = 1.28 \times 10^2$ mol^{-1} dm^3 s^{-1} (25 °C) and that *trans*-$[Ru^{VI}(L)O(X)]^{n+}$ is stable in the presence of PPh_3 (1 M) over a period of several hours at room temperature. The formation of *trans*-$[Ru^{IV}(L)O(CH_3CN)]^{2+}$ in reaction 1 was also accompanied by the generation of $O{=}PPh_3$ as another reaction product, identified by its IR absorption bands at 712 and 1175 cm^{-1}. Groves and co-workers[17] reported that the PPh_3 reduction of *trans*-$[Ru^{VI}(TMP)O_2]$ yielded a Ru(II) complex as the isolatable product. These workers postulated an $[Ru^{IV}(TMP)O]$ intermediate, which is unstable toward disproportionation into Ru(II) and Ru(VI). However, Ru^{IV}=O complexes with neutral amine ligands, such as *trans*-$[Ru^{IV}(L)O(X)]^{n+}$ and $[Ru^{IV}(trpy)(bpy)O]^{2+}$, do not appear to disproportionate in solution. Thus the nonlabile ligands have a dramatic effect on both the stability and reactivity of the Ru^{IV}=O system. A neutral Ru^{IV}=O complex has so far not been reported. The chloride ligand in *trans*-$[Ru^{IV}(L)O(Cl)]^+$ mostly came from the reduction of ClO_4^- ion by PPh_3. *trans*-$[Ru^{IV}(14\text{-TMC})O(Cl)]ClO_4$ has been characterized by X-ray crystallography.[8a] Reaction of *trans*-$[Ru^{VI}(16\text{-TMC})O_2][ClO_4]_2$ with PPh_3 in acetone gave a blue solution. Attempts to isolate pure *trans*-$[Ru^{IV}(16\text{-TMC})O(Cl)]ClO_4$ out were unsuccessful, and the product was usually found to contaminate with some unidentified blue species.

The second method for *trans*-$[Ru^{IV}(L)O(X)]^{n+}$ involves the H_2O_2 oxidation of *trans*-$[Ru^{III}(L)(OH_2)_2]^{3+}$ in the presence of X^-. *trans*-$[Ru^{IV}(L)O(N_3)]ClO_4$ and *trans*-$[Ru^{IV}(L)O(NCO)]ClO_4$ were prepared accordingly. It is likely that *trans*-$[Ru^{III}(L)(OH_2)_2]^{3+}$ undergoes anation prior to the oxidation process

$$trans\text{-}[Ru^{III}(L)(OH_2)_2]^{3+} + X^- \rightarrow trans\text{-}[Ru^{III}(L)(OH_2)(X)]^{2+} \xrightarrow{[O]} trans\text{-}[Ru^{IV}(L)O(X)]^+$$

Yukawa et al.[18] recently reported the isolation of *trans*-$[Ru^{IV}(py)_4O(Cl)]ClO_4$ through H_2O_2 oxidation of *trans*-$[Ru^{II}(py)_4(NO)Cl][ClO_4]_2$.

A *trans*-dioxoruthenium(V) complex can be prepared by electrosynthesis from the parent *trans*-$[Ru^{VI}(L)O_2]^{2+}$. Solid *trans*-$[Ru^{V}(14\text{-TMC})O_2]ClO_4$ was found to be very hygroscopic. For this reason, no attempt was made to isolate *trans*-$[Ru^{VI}(15\text{-TMC})O_2]ClO_4$ and *trans*-$[Ru^{V}(16\text{-TMC})O_2]ClO_4$. *trans*-$[Ru^{V}(TMEA)_2O_2]^+$ was unstable in acetonitrile and slowly turned into an unidentified green substance at room temperature.

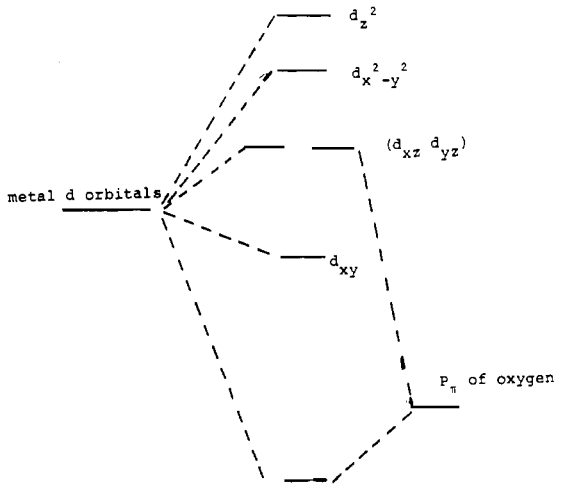

Figure 2. Simplified molecular orbital diagram illustrating the p_π(O) and d_π(M) orbital interaction of the "M=O" system.

The results of molar conductivity measuremnts are available as supplementary materials (Table S1). With the exception of *trans*-$[Ru^{IV}(L)O(Cl)]ClO_4$ in water, the findings are in accord with the chemical formulation of the compounds, that is, 120–130 and 240–253 Ω^{-1} mol^{-1} cm^2 for 1:1 and 1:2 electrolytes, respectively. The measured molar conductivity of 243 Ω^{-1} mol^{-1} cm^2 for *trans*-$[Ru^{IV}(14\text{-TMC})O(Cl)]ClO_4$ in water suggests that it exists as a 1:2 electrolyte in aqueous medium. Presumably, this complex undergoes rapid solvolysis in water

$$trans\text{-}[Ru^{IV}(14\text{-TMC})O(Cl)]^+ + H_2O \rightarrow trans\text{-}[Ru^{IV}(14\text{-TMC})O(OH_2)]^{2+} + Cl^- \quad (3)$$

The presence of free Cl^- ion in solution was confirmed by the immediate formation of white AgCl precipitate upon addition of silver toluene-*p*-sulfonate to an aqueous solution of *trans*-$[Ru^{IV}(14\text{-TMC})O(Cl)]^+$. Measurements on the Cl^- concentration with an ion-selective electrode also indicated that the equilibrium lies far to the right in reaction 3. *trans*-$[Ru^{IV}(15\text{-TMC})O(Cl)]ClO_4$ and *trans*-$[Ru^{IV}(TMEA)_2O(Cl)]ClO_4$ behave in a similar manner.

All solid *trans*-$[Ru^{IV}(L)O(X)]^{n+}$ complexes are stable to room light at room temperature; they do not appear to decompose even upon storage for 1 week. Though *trans*-$[Ru^{VI}(14\text{-TMC})O_2][ClO_4]_2$ had been obtained in crystalline form, the crystals gradually decomposed either in solution or in the dry state to give a straw-colored amorphous solid first and finally a black solid. We suggest that the instability of trans-$[Ru^{VI}(14\text{-TMC})O_2][ClO_4]_2$ may be due to the large steric repulsive effect between the *N*-methyl groups and the proximal oxo ligands. In this regard, enlargement of the macrocyclic ring by replacement of 14-TMC with 15-TMC or 16-TMC might possibly relieve the steric constraint and hence increase the stability of the dioxo-Ru(VI) species. Accordingly, *trans*-$[Ru^{VI}(15\text{-TMC})O_2][ClO_4]_2$ and *trans*-$[Ru^{VI}(16\text{-TMC})O_2][ClO_4]_2$ are stable to room light for 2–3 h and appear to be indefinitely stable at 0 °C under dark conditions.

Electronic Configuration of Ruthenium Oxo Complexes. The results of magnetic susceptibility measurements are available as supplementary material (Table S2).

The electronic configuration of Ru=O complexes can be rationalized on the basis of the simplified molecular orbital energy scheme (Figure 2) after the works of Ballhausen, Gray, and Hare.[19] Because of the p_π(O) and d_π(Ru) orbital overlap, the d_{xz} and d_{yz} orbitals, here denoted as d_{π^*}, are antibonding in nature

(16) (a) Wong, K. Y. Ph.D. Thesis, University of Hong Kong, 1986. (b) Wong, K. Y.; Che, C. M.; Anson, F. C. *Inorg. Chem.* **1987**, *26*, 737.
(17) Groves, J. T.; Quinn, R. *J. Am. Chem. Soc.* **1985**, *107*, 5790.
(18) Yukawa, Y.; Aoyagi, K.; Kurihara, M.; Shirai, K.; Shimiza, K.; Mukaida, M.; Takeuchi, T.; Kakihana, H. *Chem. Lett.* **1985**, 283.
(19) (a) Ballhausen, C. J.; Gray, H. B. *Inorg. Chem.* **1962**, *1*, 111. (b) Gray, H. B.; Hare, C. R. *Inorg. Chem.* **1962**, *1*, 363.

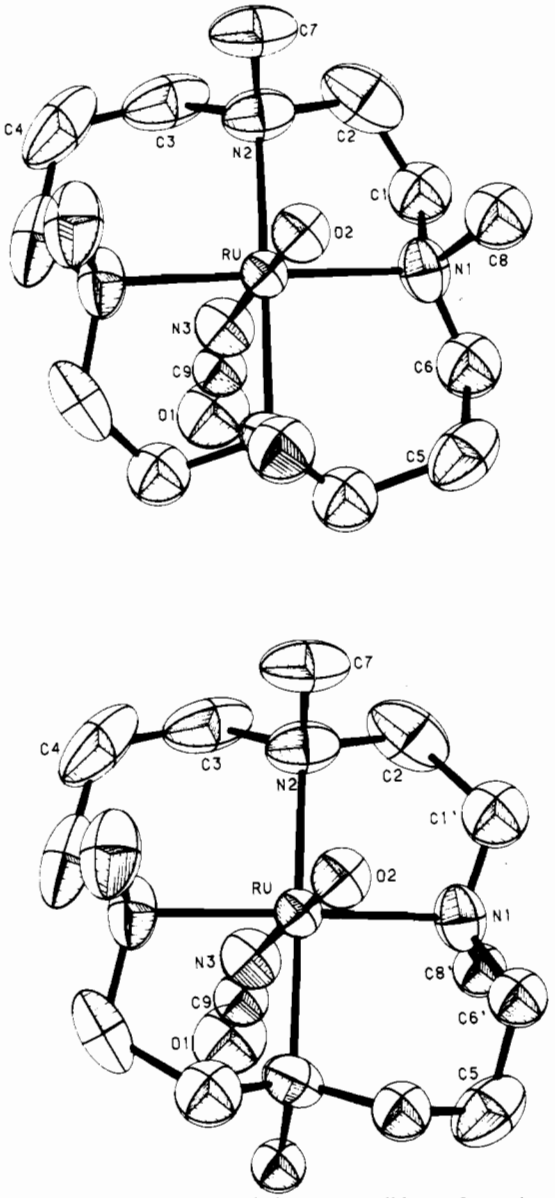

Figure 3. ORTEP drawings of the two possible conformations of the *trans*-$[Ru^{IV}(14\text{-TMC})O(NCO)]^+$ cation with the atomic numbering scheme.

and higher in energy than the d_{xy} orbital. On this basis, d^4 Ru^{IV}=O and d^3 Ru^{V}=O complexes are expected to have the $(d_{xy})^2(d_{xz})^1(d_{yz})^1$ and $(d_{xy})^2(d_{\pi^*})^1$ ground-state electronic configurations, respectively. All Ru^{IV}=O complexes including *trans*-$[Ru^{IV}(py)_4O(Cl)]ClO_4$ and $[Ru^{IV}(trpy)(bpy)O](ClO_4)_2$ are paramagnetic; their measured μ_{eff} of 2.70–2.95 μ_B (Table S2) are characteristic of the spin-only value for two unpaired electrons.[3c,18] For *trans*-$[Ru^{V}(14\text{-TMC})O_2]ClO_4$, its μ_{eff} of 1.94 μ_B (Table S2) at room temperature is in accord with the formulation of one unpaired electron in the d_{π}^* orbitals.

Structure Description of Ruthenium Oxo Complexes. Figure 3 shows the ORTEP drawings of the two possible conformations of the *trans*-$[Ru^{IV}(14\text{-TMC})O(NCO)]^+$ cation and the atomic numbering scheme. The Ru, C(4), C(5), N(3), C(9), O(1), and O(2) atoms all lie on the crystallographic mirror plane. The coordination geometry about the Ru atom is distorted octahedral with the metal atom displaced slightly from the mean plane of the four equatorial N atoms (mean deviation, 0.061 Å) toward the axial oxygen atom. The N(3)–Ru–O axis is slightly bent (∠N(3)–Ru–O(2) = 178.2°); similar findings on *trans*-$[Ru^{IV}(14\text{-TMC})O(CH_3CN)]^{2+}$ (∠N(CH_3CN)–Ru–O = 177.6°) and *trans*-$[Ru^{IV}(14\text{-TMC})O(Cl)]^+$ (∠Cl–Ru–O = 177.2) have also been observed.[8a,b] The distortion of the X–Ru–O axis in *trans*-$[Ru^{IV}(14\text{-TMC})O(X)]^{n+}$ system is possibly a consequence

Table III. Comparison of the Ru–X (Axial Ligand) and Ru–N (Macrocyclic Amine) Distances of *trans*-$[Ru^{VI}(L)O_2]^{2+}$ (L = 15-TMC, 16-TMC) and *trans*-$[Ru^{IV}(14\text{-TMC})O(X)]^{n+}$ (n = 1, X = Cl, NCO; n = 2, X = CH_3CN) Complexes

complex	Ru–X, Å	Ru–N, Å
trans-$[Ru^{VI}(15\text{-TMC})O_2][ClO_4]_2$		2.17 (1)–2.22 (3)[a]
trans-$[Ru^{VI}(16\text{-TMC})O_2][ClO_4]_2$		2.21 (1)–2.24 (1)[a]
trans-$[Ru^{IV}(14\text{-TMC})O(CH_3CN)][PF_6]_2$	2.149 (6)[b]	2.08 (5)–2.14 (1)[b]
trans-$[Ru^{IV}(14\text{-TMC})O(Cl)]ClO_4$	2.505 (3)[b]	2.07 (2)–2.16 (2)[b]
trans-$[Ru^{IV}(14\text{-TMC})O(NCO)]ClO_4$	2.119 (6)	2.132 (5)–2.134 (5)

[a] Reference 8b. [b] Reference 8a.

Table IV. Ru=O Bond Distances and Stretching Frequencies in Ruthenium Oxo Complexes

complexes	d(Ru=O), Å	ν(Ru=O), cm^{-1}
trans-$[Ru^{VI}(14\text{-TMC})O_2][ClO_4]_2$		850
trans-$[Ru^{VI}(15\text{-TMC})O_2][ClO_4]_2$	1.718 (5)[a]	855
trans-$[Ru^{VI}(16\text{-TMC})O_2][ClO_4]_2$	1.705 (7)[a]	860
trans-$[Ru^{VI}(TMEA)_2O_2][ClO_4]_2$		860
trans-$[Ru^{VI}(bpy)_2O_2][ClO_4]_2$		850[c]
trans-$[Ru^{VI}(TMP)O_2]$		821[b]
trans-$[Ru^{IV}(trpy)(bpy)O][ClO_4]_2$		792[d]
trans-$[Ru^{IV}(py)_4O(Cl)]ClO_4$	1.862 (8)[e]	~800[e]
trans-$[Ru^{IV}(14\text{-TMC})O(CH_3CN)][PF_6]_2$	1.765 (5)[f]	~815
trans-$[Ru^{IV}(14\text{-TMC})O(Cl)]ClO_4$	1.765 (5)[f]	~815
trans-$[Ru^{IV}(14\text{-TMC})O(NCO)]ClO_4$	1.765 (5)	~815
trans-$[Ru^{IV}(14\text{-TMC})O(N_3)]ClO_4$	1.765 (5)[g]	~815
trans-$[Ru^{IV}(15\text{-TMC})O(CH_3CN)][ClO_4]_2$		~820
trans-$[Ru^{IV}(15\text{-TMC})O(Cl)]ClO_4$		~820
trans-$[Ru^{IV}(15\text{-TMC})O(N_3)]ClO_4$		~820
trans-$[Ru^{IV}(TMEA)_2O(Cl)]ClO_4$		~820

[a] Reference 8a. [b] Reference 11. [c] Reference 15. [d] Reference 3. [e] Reference 18. [f] Reference 8a. [g] Che, C. M., unpublished result

of the nonbonded repulsive interactions of the N–CH_3 groups with the axial ligand X. The two conformations of the 14-TMC ligand in *trans*-$[Ru^{IV}(14\text{-TMC})O(NCO)]^+$ cation are the "four up (down)" (*R*,*S*,*R*,*S*) and "two up, two down" (*R*,*R*,*S*,*S*)/(*S*,*S*,*R*,*R*) sets of nitrogen atom configurations; in the latter case, two adjacent N–CH_3 groups are cis to the Ru–O bond. The (*R*,*S*,*R*,*S*) configuration of the 14-TMC ligand has been found in *trans*-$[Ru^{IV}(14\text{-TMC})O(CH_3CN)][ClO_4]_2$.[8a] Other possible conformations, such as the "three up, one down" (*R*,*S*,*R*,*R*) set of nitrogen atom configurations is observed in *trans*-$[Ru^{IV}(14\text{-TMC})O(Cl)]^+$.[8a] We believe that the observed orientations of the N–CH_3 groups of the 14-TMC ligand in the *trans*-$[Ru^{IV}(14\text{-TMC})O(X)]^{n+}$ system may not be related to the nature of the axial ligand X but rather to the reaction conditions employed for the preparation and isolation of the complexes. The five- and six-membered chelate rings of *trans*-$[Ru^{IV}(14\text{-TMC})O(NCO)]^+$ have gauche and chair conformations, respectively. The average Cl–O distance and O–Cl–O angle in the perchlorate group are respectively 1.42 ± 0.002 Å and 109.0 ± 2.5°.

The Ru–N (equatorial amine) bond distances in the Ru(IV) and Ru(VI) oxo complexes are similar and fall within 2.10–2.2 Å (Table III), which are comparable to those found in other ruthenium macrocyclic amine complexes, such as *cis*- and *trans*-$[Ru(14aneN_4)Cl_2]^+$.[20,21] The Ru–N(NCO) bond distance of 2.119 (6) Å is comparable to the Ru–N(CH_3CN) bond distance (2.149 (6) Å) in *trans*-$[Ru^{IV}(14\text{-TMC})O(CH_3CN)]^{2+}$ (Table III). For O=Ru^{IV}—X complexes, the Ru–X bonds are abnormally long, indicating the strong trans effect of the oxo ligand.

Effect of Ligand and Oxidation State on the Ru=O Bond. Table IV summarizes the Ru=O bond distances and ν(Ru=O)

(20) Che, C. M.; Kwong, S. S.; Poon, C. K.; Lai, T. F.; Mak, T. C. W. *Inorg. Chem.* **1985**, *24*, 1359.
(21) Walker, D. D.; Taube, H. *Inorg. Chem.* **1981**, *20*, 2828.

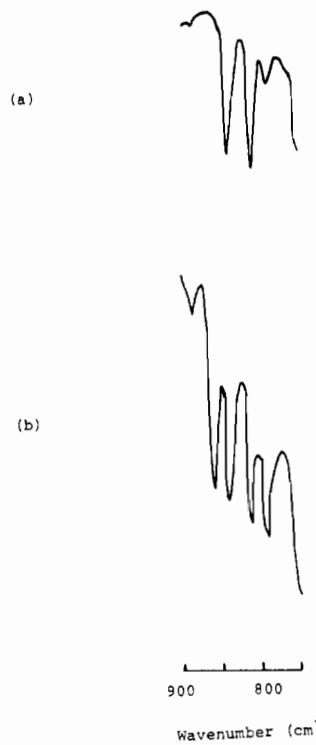

Figure 4. IR spectra of (a) *trans*-$[Ru^{III}(14\text{-}TMC)Cl_2]ClO_4$ and (b) *trans*-$[Ru^{V}(14\text{-}TMC)O_2]ClO_4$ in the 750–900-cm^{-1} region.

stretching frequencies of *trans*-$[Ru^{VI}(bpy)_2O_2][ClO_4]_2$,[15] *trans*-$[Ru^{VI}(TMP)O_2]$,[11] *trans*-$[Ru^{IV}(py)_4O(Cl)]ClO_4$,[18] $[Ru^{IV}(trpy)(bpy)O][ClO_4]_2$,[3c] and the ruthenium tertiary amine oxo complexes. Assignment of the Ru=O stretch in *trans*-$[Ru^{IV}(L)O(X)]^{n+}$ is only tentative since the tertiary amine ligand also absorbs in the 800–750-cm^{-1} region. A careful examination of the IR spectra of *trans*-$[Ru^{III}(14\text{-}TMC)Cl_2]Cl$, *trans*-$[Ru^{IV}(14\text{-}TMC)O(CH_3CN)][ClO_4]_2$, and *trans*-$[Ru^{IV}(14\text{-}TMC)O(Cl)]ClO_4$ showed the Ru(IV) complexes have an extra absorption band at ~810 cm^{-1} that is possibly the Ru=O stretch. For the d^3 *trans*-$[Ru^{V}(14\text{-}TMC)O_2]ClO_4$ system $[(d_{xy})^2(d_{\pi^*})^1]$, Jahn–Teller distortion along the *x*,*y* axis will split the degenarcy of the d_π^* orbitals. Two IR-active Ru=O stretches are expected. Figure 4 shows the IR spectrum of *trans*-$[Ru^{V}(14\text{-}TMC)O_2]ClO_4$ in the 750–900-cm^{-1} region. The intense bands at 840–860 cm^{-1} are likely due to the Ru=O stretches. For the dioxoruthenium(VI) system, only one intense IR-active ν_{as}(Ru=O) stretch is found, and the assignment has been discussed previously.[10,14,15]

A direct comparison of the Ru=O stretching frequencies (840–860 cm^{-1} vs. 810–790 cm^{-1}) and bond distances (1.70–1.71 Å vs. 1.765 Å) between *trans*-$[Ru^{VI}(L)O_2]^{2+}$ and *trans*-$[Ru^{IV}(L)O(X)]^{n+}$ complexes indicates that the Ru=O bond is weaker in the latter system. This finding is in accord with the bonding picture because putting two electrons into the antibonding d_π^* orbitals should weaken the Ru=O bond [Ru(VI), $(d_{xy})^2$; Ru(IV), $(d_{xy})^2(d_{xz})^1(d_{yz})^1$]. Enlargement of the macrocyclic ring size from 14-TMC to 16-TMC does not appear to perturb the Ru=O bond as the Ru=O distances for *trans*-$[Ru^{VI}(15\text{-}TMC)O_2]ClO_4$ and *trans*-$[Ru^{VI}(16\text{-}TMC)O_2][ClO_4]_2$ are similar (15-TMC, 1.718 (5) Å; 16-TMC, 1.705 (7) Å). For the *trans*-$[Ru^{IV}(14\text{-}TMC)O(X)]^{n+}$ system, the measured Ru=O bond distances are all 1.765 Å, independent of the charge of the metal complex and nucleophilicity of the axial ligand. Thus axial ligation does not perturb the Ru=O bond, reflecting that the primary bonding interaction in the X—Ru^{IV}=O system is the d_π(Ru) and p_π(O) orbital overlap. Accordingly, the Ru–X bonds in *trans*-$[Ru^{IV}(L)O(X)]^{n+}$ complexes are all abnormally long (Table III).

Replacement of the equatorial amine ligand from the σ-saturated to the π-aromatic type has a dramatic effect on the Ru=O bond. In the Ru^{IV}=O system, *d*(Ru=O) for *trans*-$[Ru^{IV}(py)_4O(Cl)]^+$ (1.862 Å)[18] is ~0.1 Å longer than that for *trans*-$[Ru^{IV}(14\text{-}TMC)O(Cl)]^+$, indicating that the former system has a weaker Ru=O bond. For the *trans*-dioxoruthenium(VI) system, no structural work has been reported on *trans*-$[Ru^{VI}(bpy)_2O_2]^{2+}$ and *trans*-$[Ru^{VI}(TMP)O_2]$. However, the ν_{as}(Ru=O) stretching frequency for *trans*-$[Ru^{VI}(TMP)O_2]$ is ~821 cm^{-1}, which is much lower *than the 850–860-cm^{-1} value found for those complexes containing neutral amine ligands*. As shown later in the text, *trans*-$[Ru^{VI}(TMP)O_2]$ is a better epoxidation reagent than *trans*-$[Ru^{VI}(TMC)O_2]^{2+}$, in accord with the picture that the latter system has a stronger Ru=O bond. The weakening of the Ru=O bond by the π-saturated ligand, such as pyridine or the porphyrinate dianion, could be attributed to the repulsive coulombic interactions of the ligand p_π electrons and the p_π–d_π electrons of the Ru=O bond. The observation of this ligand effect on the Ru=O bond is important because this will give guidelines in the future design of Ru=O system for uses in chemoselective oxidation reactions. We suggest that a short Ru=O bond will favor hydride/hydrogen atom abstraction and this can be achieved with highly oxidizing Ru(VI)–dioxo complexes of tertiary amine. For selective epoxidation reaction, one must look for those complexes having long and hence weak Ru=O bonds. The Ru^{IV}=O complexes containing dianionic π-unsaturated ligands are the best candidates.

Table V. Formal Potentials of Ru(VI)/Ru(IV) and Ru(IV)/Ru(III) Couples of Ruthenium Oxo Complexes at pH 1.0

couples	$E_f°$, V vs. NHE
trans-$[Ru^{VI}(14\text{-}TMC)O_2]^{2+}$/ *trans*-$[Ru^{IV}(14\text{-}TMC)O(OH_2)]^{2+}$ [a]	0.90
trans-$[Ru^{VI}(15\text{-}TMC)O_2]^{2+}$/ *trans*-$[Ru^{IV}(15\text{-}TMC)O(OH_2)]^{2+}$	0.89
trans-$[Ru^{VI}(16\text{-}TMC)O_2]^{2+}$/ *trans*-$[Ru^{IV}(16\text{-}TMC)O(OH_2)]^{2+}$	0.90
trans-$[Ru^{VI}(TMEA)_2O_2]^{2+}$/ *trans*-$[Ru^{IV}(TMEA)_2O(OH_2)]^{2+}$	0.91
trans-$[Ru^{VI}(bpy)_2O_2]^{2+}$/ *trans*-$[Ru^{IV}(bpy)_2O(OH_2)]^{2+}$ [b]	1.25
trans-$[Ru^{IV}(14\text{-}TMC)O(OH_2)]^{2+}$/ *trans*-$[Ru^{III}(14\text{-}TMC)(OH)(OH_2)]^{2+}$ [a]	0.60
trans-$[Ru^{IV}(15\text{-}TMC)O(OH_2)]^{2+}$/ *trans*-$[Ru^{III}(15\text{-}TMC)(OH)(OH_2)]^{2+}$	0.58
trans-$[Ru^{IV}(16\text{-}TMC)O(OH)_2]^{2+}$/ *trans*-$[Ru^{III}(16\text{-}TMC)(OH)(OH_2)]^{2+}$	0.57
trans-$[Ru^{IV}(TMEA)_2O(OH_2)]^{2+}$/ *trans*-$[Ru^{IV}(TMEA)_2(OH)(OH_2)]^{2+}$	0.58
trans-$[Ru^{IV}(bpy)_2O(OH_2)]^{2+}$/ *trans*-$[Ru^{III}(bpy)_2(OH)(OH_2)]^{2+}$ [b]	1.12

[a] Reference 6. [b] Reference 15.

Effect of Ligand on the Oxidation Potentials of Ru=O Complexes. We have previously shown that at pH 1.1, *trans*-$[Ru^{VI}(bpy)O_2]^{2+}$ [15] and *trans*-$[Ru^{VI}(14\text{-}TMC)O_2]^{2+}$ [10] exhibit a reversible two-proton two-electron Ru(VI)/Ru(IV) couple:

$$trans\text{-}[Ru^{VI}(L)O_2]^{2+} + 2H^+ + 2e^- \rightarrow trans\text{-}[Ru^{IV}(L)O(OH_2)]^{2+}$$

L = $(bpy)_2$, 14-TMC, 15-TMC, 16-TMC, $(TMEA)_2$

Typical cyclic voltammograms for *trans*-$[Ru^{VI}(16\text{-}TMC)O_2][ClO_4]_2$ in 0.1 M $HClO_4$ and acetonitrile are shown in Figure 5. In acetonitrile, *trans*-$[Ru^{VI}(L)O_2]^{2+}$ undergoes a reversible one-electron-reduction process:

$$trans\text{-}[Ru^{VI}(L)O_2]^{2+} + e^- \rightarrow trans\text{-}[Ru^{V}(L)O_2]^{+}$$

Table V summarizes the oxidation potential of Ru(VI)– and Ru(IV)–oxo complexes. Enlargement of the hole size from the 14- to 16-member ring does not affect the $E_{1/2}$ values of *trans*-$[Ru^{VI}(L)O_2]^{2+}$/*trans*-$[Ru^{IV}(L)O(OH_2)]^{2+}$ and *trans*-$[Ru^{VI}(L)O_2]^{2+}$/*trans*-$[Ru^{V}(L)O_2]^{+}$ redox couples. However, replacement of the σ-saturated tertiary amine by the π-aromatic one has a dramatic effect on the oxidation potential of the Ru(VI)–dioxo complexes. *trans*-$[Ru^{VI}(bpy)_2O_2]^{2+}$ is over 340 mV more oxidizing than *trans*-$[Ru^{VI}(14\text{-}TMC)O_2]^{2+}$ in aqueous medium. Similar ligand effects on the reduction potential of

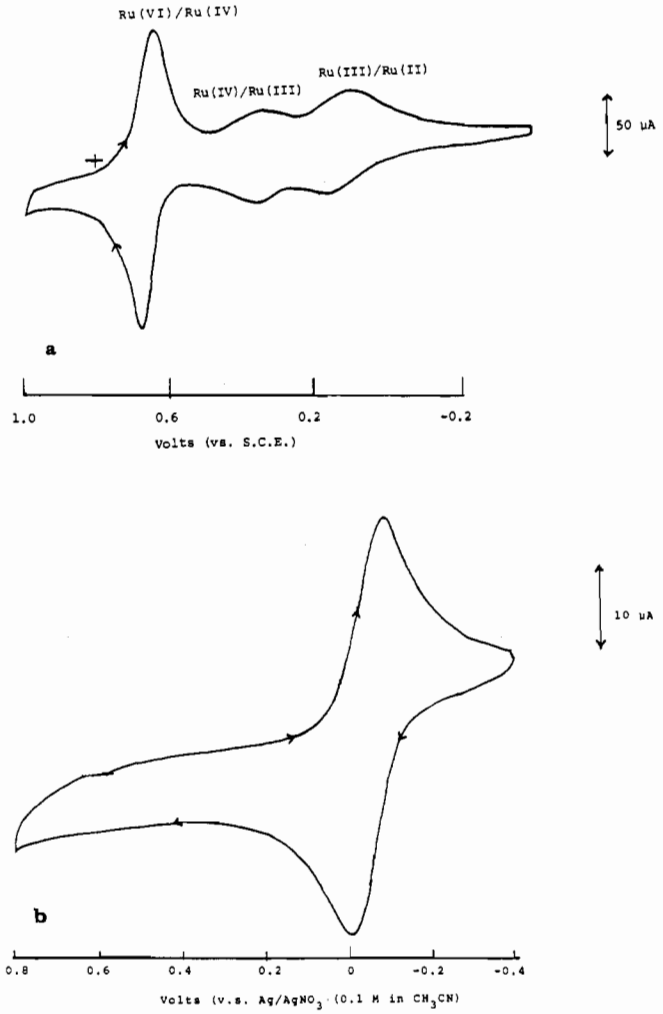

Figure 5. Cyclic voltammograms for *trans*-$[Ru^{VI}(16\text{-TMC})O_2][ClO_4]_2$ (~1 mM) in (a) 0.1 M $HClO_4$ and (b) 0.1 M $[Bu_4N]ClO_4$ in acetonitrile. Conditions: working electrode, pyrolytic graphite; scan rate, 50 mV s^{-1}.

Ru^{IV}=O complexes have also been found. For example, the $E_{1/2}$ value for $[Ru^{IV}(bpy)_2(py)O]^{2+}/[Ru^{III}(bpy)_2(py)(OH_2)]^{3+}$ couple is 0.99 V vs. SCE[3a] (1 M acid) whereas the corresponding value for *trans*-$[Ru^{IV}(14\text{-TMC})O(OH_2)]^{2+}$/*trans*-$[Ru^{III}(14\text{-TMC})(OH_2)_2]^{3+}$ couple is 0.36 V vs. SCE at pH 1.1.[10] Thus the π-aromatic amine, although oxidation resistant upon complexation, destabilizes the high-valent ruthenium oxo system, and is a poorer σ-donor than the σ-saturated tertiary amine.

For *trans*-$[Ru^{IV}(L)O(X)]^+$ system (L = 14-TMC, 15-TMC, $(TMEA)_2$; X = Cl, NCO, N_3), the electrochemical oxidation of Ru(IV) to Ru(V) at potential of 0.7–1.1 V (vs. $AgNO_3$ (0.1 M)/Ag) is a simple and reversible one-electron process.[16] A summary of the $E_{1/2}$ values of the Ru(V)/Ru(IV) couples is shown in Table VI. The $E_{1/2}$ value is insensitive to the nature of tertiary amine; however, it varies with the nature of the axial ligand (X) and decreases with X = Cl > NCO > N_3, indicating that the electrode reaction is the metal-centered oxidation of Ru(IV) to Ru(V). No Ru(V)/Ru(IV) couple has yet been observed for *trans*-$[Ru^{IV}(L)O(CH_3CN)]^{2+}$ system. The *trans*-$[Ru^{IV}(L)O(X)]^+$ complexes are all electrocatalysts for the oxidation of alcohol.[8b,16] Figure 6 illustrates the cyclic voltammograms of *trans*-$[Ru^{IV}(14\text{-TMC})O(NCO)]^+$ in the presence and absence of 100 mM benzyl alcohol. Catalytic oxidative current at the same potential of the Ru(V)/Ru(IV) couple was found in all the *trans*-$[Ru^{IV}(L)O(X)]^+$ complexes. The rate of alcohol oxidation by *trans*-$[(14\text{-TMC})O(X)]^{2+}$ decreases with X = Cl > NCO > N_3.[16] Thus,

Table VI. Formal Potentials of Ru(V)/Ru(IV) Couples in 0.1 M $[Bu_4N]BF_4$ in Acetonitrile Solution

couples	$E_f°$, V vs. $Cp_2Fe^{+/0}$
trans-$[Ru(14\text{-TMC})O(Cl)]^{2+/+}$	1.10
trans-$[Ru(15\text{-TMC})O(Cl)]^{2+/+}$	1.10
trans-$[Ru(TMEA)_2O(Cl)^{2+/+}$	1.06
trans-$[Ru(14\text{-TMC})O(NCO)]^{2+/+}$	0.89
trans-$[Ru(14\text{-TMC})O(N_3)]^{2+/+}$	0.72
trans-$[Ru(15\text{-TMC})O(N_3)]^{2+/+}$	0.71

[a] Glassy-carbon working electrode.

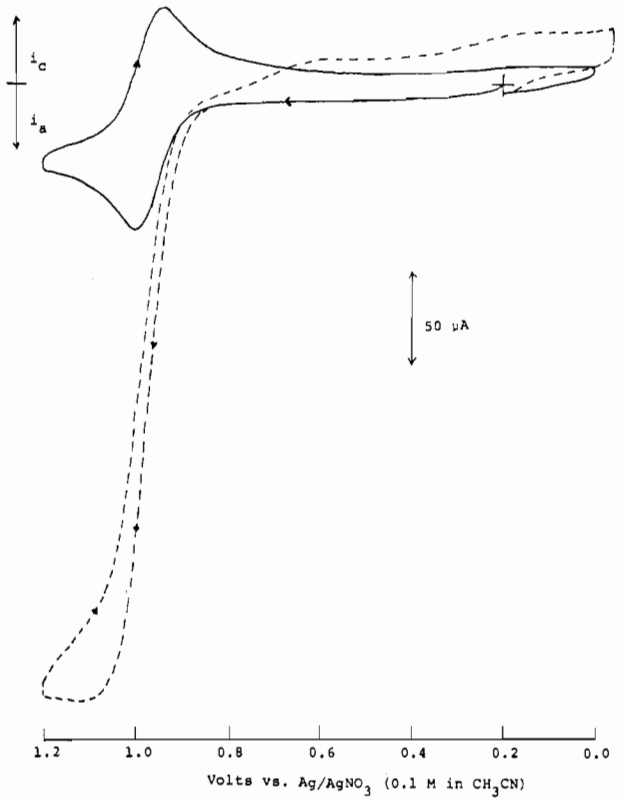

Figure 6. Cyclic voltammograms of 2.4 mM of *trans*-$[Ru^{IV}(14\text{-TMC})O(NCO)]^+$ in acetonitrile with $[Bu_4N]BF_4$ (0.1 M) as supporting electrolyte showing the catalytic current upon the addition of benzyl alcohol: (—) absence of alcohol; (---) 100 mM benzyl alcohol added. Conditions: working electrode, glassy carbon; scan rate, 100 mV s^{-1}.

axial ligand ligation plays a substantial role in affecting the redox reactivities of the Ru^V=O complexes.

UV–Vis Spectroscopy of Ru=O Complexes. There are two types of electronic transitions in the "Ru=O" system, the ligand-field ($d_{xy} \rightarrow d_{\pi^*}$) and ligand to metal ($P_\pi(O) \rightarrow d_\pi(M)$) charge transfer (LMCT).[6,15,19,22] Figure 7 shows the optical spectra of *trans*-$[Ru^{VI}(16\text{-TMC})O_2]^{2+}$, *trans*-$[Ru^{VI}(15\text{-TMC})O_2]^{2+}$, and *trans*-$[Ru^{VI}(14\text{-TMC})O_2]^{2+}$ complexes in CH_3CN. The vibronic structured $d_{xy} \rightarrow d_{\pi^*}$ transition at 370–400 nm is a general characteristic optical spectral feature of the *trans*-dioxoruthenium(VI) system.[23] For *trans*-$[Ru^{VI}(L)O_2]^{2+}$, the position of this band is insensitive to the nature of the equatorial amine and the macrocyclic ring size of L (14-TMC, 388 nm; 15-TMC, 377 nm; 16-TMC, 375 nm) (Table VII), in accordance with the formulation that the electronic transition occurs within the nonbonding d_{π^*} orbitals. Occupancy of one or two electrons in the d_{π^*} orbitals will lower their energy. Accordingly, the $d_{xy} \rightarrow d_{\pi^*}$ transition will be red-shifted with decreasing oxidation state of

(22) Winkler, J. R.; Gray, H. B. *Inorg. Chem.* **1985**, *24*, 346.
(23) See also: Foster, S.; Felps, S.; Johnson, L. W.; Larson, D. B.; McGlynn, S. P. *J. Am. Chem. Soc.* **1973**, *95*, 6578.

Table VII. Electronic Spectral Data for Ruthenium Oxo Complexes

complexes	solvent	λ_{max}, nm (ϵ_{max}, cm^{-1} dm^3 mol^{-1})[a]
trans-$[Ru^{VI}(14\text{-}TMC)O_2][ClO_4]_2$	0.1 M $HClO_4$	~455 (sh) (50), 388 (560), ~305 (sh) (960), 255 (10 300), 225 (12 800)
	CH_3CN	~455 (sh) (50), 388 (560), ~305 (sh) (960), 255 (11 000), 223 (15 100)
trans-$[Ru^{VI}(15\text{-}TMC)O_2][ClO_4]_2$	0.1 M $HClO_4$	~430 (sh) (50), 377 (540), ~325 (sh) (1700), 276 (12 800), 235 (16 000)
	CH_3CN	~430 (sh) (50), 377 (550), ~325 (sh) (1800), 276 (14 000), 235 (18 000)
trans-$[Ru^{VI}(16\text{-}TMC)O_2][ClO_4]_2$	CH_3CN	425 (sh) (80), 375 (670), 304 (20 200), 257 (14 000)
trans-$[Ru^{VI}(TMEA)_2O_2][ClO_4]_2$	0.1M $HClO_4$	~430 (sh) (50), 385 (520), 280 (14 000), 235 (20 500)
	CH_3CN	~430 (sh) (50), 385 (530), 282 (14 500), 235 (21 000)
trans-$[Ru^{V}(14\text{-}TMC)O_2]^+$	CH_3CN	~525 (sh) (20), 422 (240), 295 (5700), 210 (9000)
trans-$[Ru^{V}(15\text{-}TMC)O_2]^+$	CH_3CN	~530 (sh) (20), 420 (260), 295 (5000), 230 (7300)
trans-$[Ru^{V}(16\text{-}TMC)O_2]^+$	CH_3CN	~550 (sh) (~10), 448 (170), 350 (sh) (1200), 295 (5100), 240 (10 400)
trans-$[Ru^{V}(TMEA)_2O_2]^+$	CH_3CN	422 (~400), 350 (sh) (~1500), 290 (~5000), 220 (~14 000)
trans-$[Ru^{IV}(14\text{-}TMC)O(CH_3CN)](ClO_4)_2$	CH_3CN	420 (190), 290 (1600)
trans-$[Ru^{IV}(14\text{-}TMC)O(Cl)]ClO_4$	CH_3CN	460 (130), 295 (2300)
	0.1 M $HClO_4$	420 (150), 280 (1600), 210 (9800)
trans-$[Ru^{IV}(14\text{-}TMC)O(NCO)]ClO_4$	CH_3CN	460 (120), 295 (4600)
trans-$[Ru^{IV}(14\text{-}TMC)O(N_3)]ClO_4$	CH_3CN	~375 (sh) (~3000), 355 (3300)
trans-$[Ru^{IV}(15\text{-}TMC)O(CH_3CN)][ClO_4]_2$	CH_3CN	475 (170), ~360 (sh) (160), 285 (1300)
trans-$[Ru^{IV}(15\text{-}TMC)O(Cl)]ClO_4$	CH_3CN	520 (110), ~370 (sh) (170), 298 (2500)
	0.1 M $HClO_4$	480 (140), 290 (2000), 220 (10 700)
trans-$[Ru^{IV}(15\text{-}TMC)O(N_3)]ClO_4$	CH_3CN	~390 (sh) (~2900), 370 (3360)
trans-$[Ru^{IV}(TMEA)_2O(Cl)]ClO_4$	CH_3CN	560 (110), ~375 (sh) (100), 298 (2800)
	0.1 M $HClO_4$	540 (100), ~370 (sh) (110), 300 (2800), 205 (15 000)

[a] sh = shoulder. [b] Reference 6.

Table VIII. Reactions of *trans*-$[Ru^{VI}(14\text{-}TMC)O_2][PF_6]_2$ with Organic Substrates

substrates	reacn conditions: quant of complex, mol	quant of substrate, mL	temp, °C	time, h	inert atmosphere	products identified (techniques used)	mol ratio of product to complex
benzyl alcohol	1.70×10^{-4}	1	50	17		benzaldehyde (GC; GC-MS)	3.50
	1.47×10^{-4}	1	50	18	argon	benzaldehyde (GC; GC-MS)	1.71
	1.56×10^{-4}	1	25	17		benzaldehyde (GC; GC-MS)	2.50
2-propanol	1.70×10^{-5}	1	50	20	N_2	acetone (UV–vis)	
benzaldehyde	1.56×10^{-4}	1	50	18		nil (UV–vis; NMR)	
cyclohexene	1.70×10^{-4}	1	50	17		2-cyclohexen-1-one (GC; GC-MS)	0.79
	1.70×10^{-4}	1	25	17		2-cyclohexen-1-one (GC;GC-MS)	0.52
cyclohexane	1.70×10^{-4}	1	50	14 h		nil (GC)	
toluene	1.70×10^{-4}	1	50	24 h		benzyl alcohol	0.04
						benzaldehyde (GC; GC-MS)	0.10

the central metal ion. For *trans*-$[Ru^{V}(L)O_2]^+$, the $d_{xy} \rightarrow d_{\pi^*}$ transition is at a lower energy (420–450 nm) (Table VII) when compared with those of the parent Ru(VI)–oxo complexes and is independent of the macrocyclic ring size of L. For the $Ru^{IV}{=}O$ system, it is difficult to assign the ligand field transition since the optical spectra are dominated by the ligand to metal charge-transfer transitions. Recent works by Miskowski and co-workers,[24] however, revealed a vibronic structure absorption band in the 600–700-nm region in the single-crystal absorption spectrum of *trans*-$[Ru^{IV}(14\text{-}TMC)O(N_3)]ClO_4$.

For *trans*-$[Ru^{VI}(14\text{-}TMC)O_2]^{2+}$, a band at 255 nm has previously been assigned as the $p_\pi(O) \rightarrow d_\pi(Ru)$ ($e_u \rightarrow e_g$) LMCT transition.[10] A closer look at the high-energy region in the optical spectra of *trans*-$[Ru^{VI}(L)O_2]^{2+}$ system (Figure 8) reveals two intense absorption bands in the 200–300-nm region (λ_{max}/nm: 14-TMC, 225, 255; 15-TMC, 223, 255; 16-TMC, 257, 304). As the position and relative extinction coefficient of these two bands vary with the nature of the equatorial amine, these two bands have substantial $\sigma N(L) \rightarrow$ Ru(VI) charge-transfer character. In *trans*-$[Ru^{V}(L)O_2]^+$ (Figure 9), an intense band at ~290–295 nm (ϵ_{max}, 5000–6000), which is invariant to the nature of L, is likely to be the lowest energy $p_\pi(O) \rightarrow d_{\pi^*}(Ru)$ LMCT transition. Figure 8 shows the optical spectra of the *trans*-$[Ru^{IV}(14\text{-}TMC)O(X)]^{n+}$ system ($n = 2$, $X = CH_3CN$; $n = 1$, X = Cl, NCO, N_3). With the exception of *trans*-$[Ru^{IV}(L)O(N_3)]^+$, all $Ru^{IV}{=}O$ complexes exhibit an intense band at 290–295 nm, which accordings with the LMCT $p_\pi(O) \rightarrow d_{\pi^*}(Ru)$ transition. Weak absorption bands are also found in the visible region (400–600 nm); their measured low ϵ_{max} values suggest that these are ligand field transitions in nature.

(24) Miskowski, V. M., unpublished result.

Oxo Complexes of Ruthenium(IV) and -(VI) as Organic Oxidants. The oxidation of organic substrates by RuO_4 and RuO_4^- systems have been studied previously.[1] These oxidants, though powerful, usually cause undesirable side reactions. Other ruthenium oxo complexes such as $[Ru^{VI}(bpy)O_2Cl_2]$,[25] $Ba[Ru^{VI}O_3(OH)_2]$,[25] and $[Ru^{IV}(trpy)(bpy)O][ClO_4]_2$[3,26] were found to be mild oxidants. Table VIII summarizes the results of the reactions between *trans*-$[Ru^{VI}(14\text{-}TMC)O_2][Y]_2$ (Y = ClO_4, PF_6) and some organic substrates. For alcohols, it oxidizes benzyl alcohol to benzaldehyde and 2-propanol to acetone. No benzoic acid was detected by both UV–vis and NMR spectroscopy. Under the same reaction conditions as in the alcohol oxidation, treatment of benzaldehyde with *trans*-$[Ru^{VI}(14\text{-}TMC)O_2][ClO_4]_2$ also failed to give benzoic acid, indicating that *trans*-$[Ru^{VI}(14\text{-}TMC)O_2][ClO_4]_2$ *is a mild oxidant*. Under degassed conditions, the reaction stoichiometry of benzyl alcohol to *trans*-$[Ru^{VI}(14\text{-}TMC)O_2][ClO_4]_2$ is ca. 2:1, in accord with the finding that *trans*-$[Ru^{IV}(L)O(X)]^{n+}$ complexes are capable of oxidizing benzyl alcohol (see discussion below).

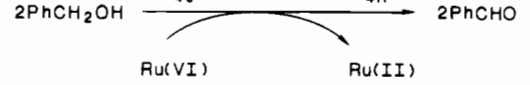

Increasing the reaction temperature from 25 to 50 °C increased the rate of the reaction.

In the presence of air, catalytic aerobic oxidation of benzyl alcohol to benzaldehyde by *trans*-$[Ru^{VI}(14\text{-}TMC)O_2]^{2+}$ was ob-

(25) Green, G.; Griffith, W. P.; Hollinshead, D. M.; Ley, S. V.; Schröder, M. *J. Chem. Soc., Perkin Trans. 1* **1984**, 681.
(26) Dobson, J. C.; Seok, W. K.; Meyer, T. J. *Inorg. Chem.* **1986**, *25*, 1513.

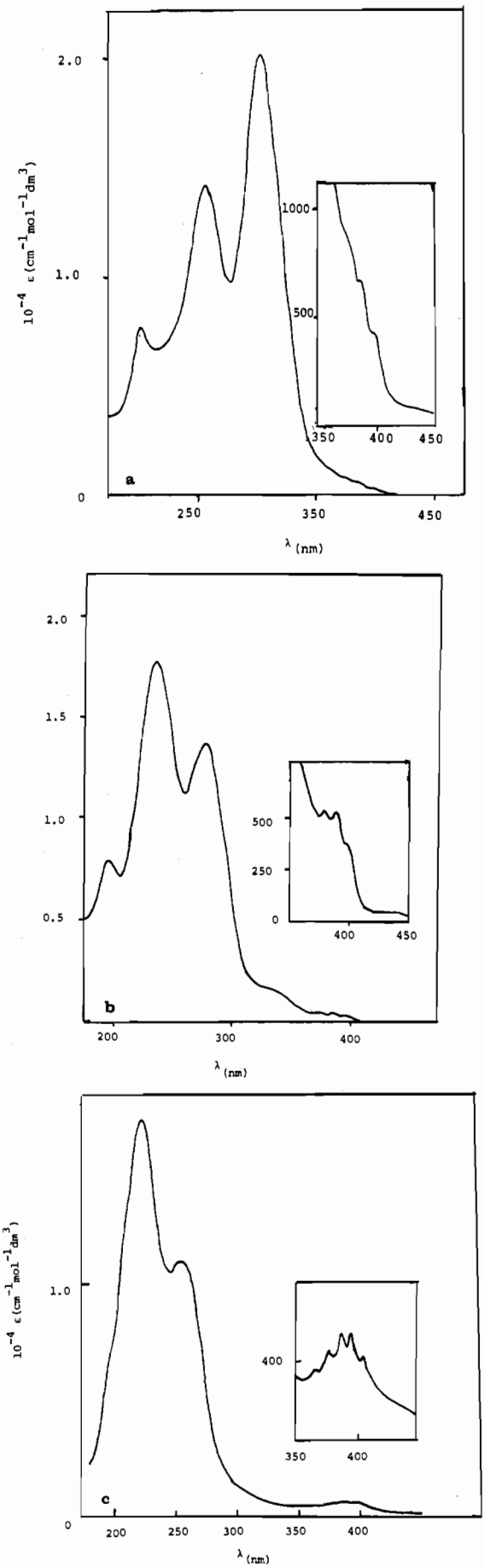

Figure 7. UV–vis spectra in CH_3CN: (a) *trans*-$[Ru^{VI}(16\text{-}TMC)O_2]^{2+}$; (b) *trans*-$[Ru^{VI}(15\text{-}TMC)O_2]^{2+}$; (c) *trans*-$[Ru^{VI}(14\text{-}TMC)O_2]^{2+}$.

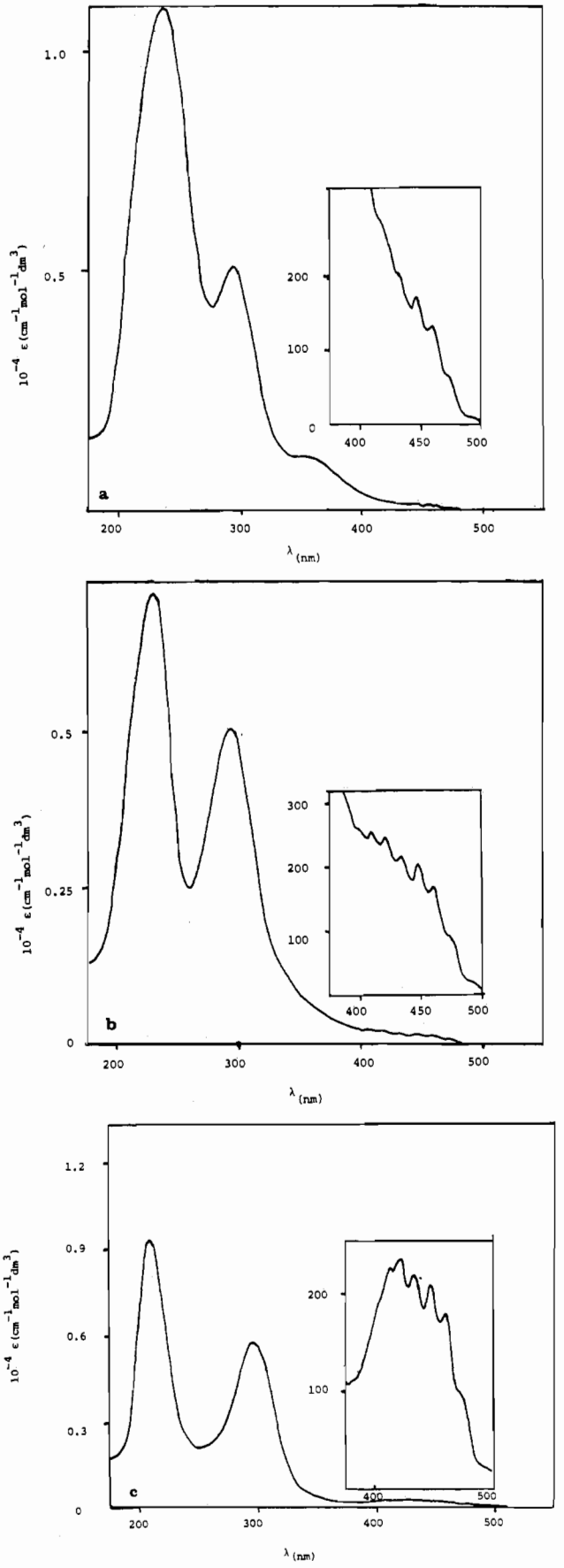

Figure 8. UV–vis spectra in CH_3CN: (a) *trans*-$[Ru^{V}(16\text{-}TMC)O_2]^{+}$; (b) *trans*-$[Ru^{V}(15\text{-}TMC)O_2]^{+}$; (c) *trans*-$[Ru^{V}(14\text{-}TMC)O_2]^{+}$.

served. The turnover number was 3.5 after 17 h (at 50 °C). In the absence of the metal complex, only a trace amount of benzaldehyde was detected. Table IX lists the results on similar studies

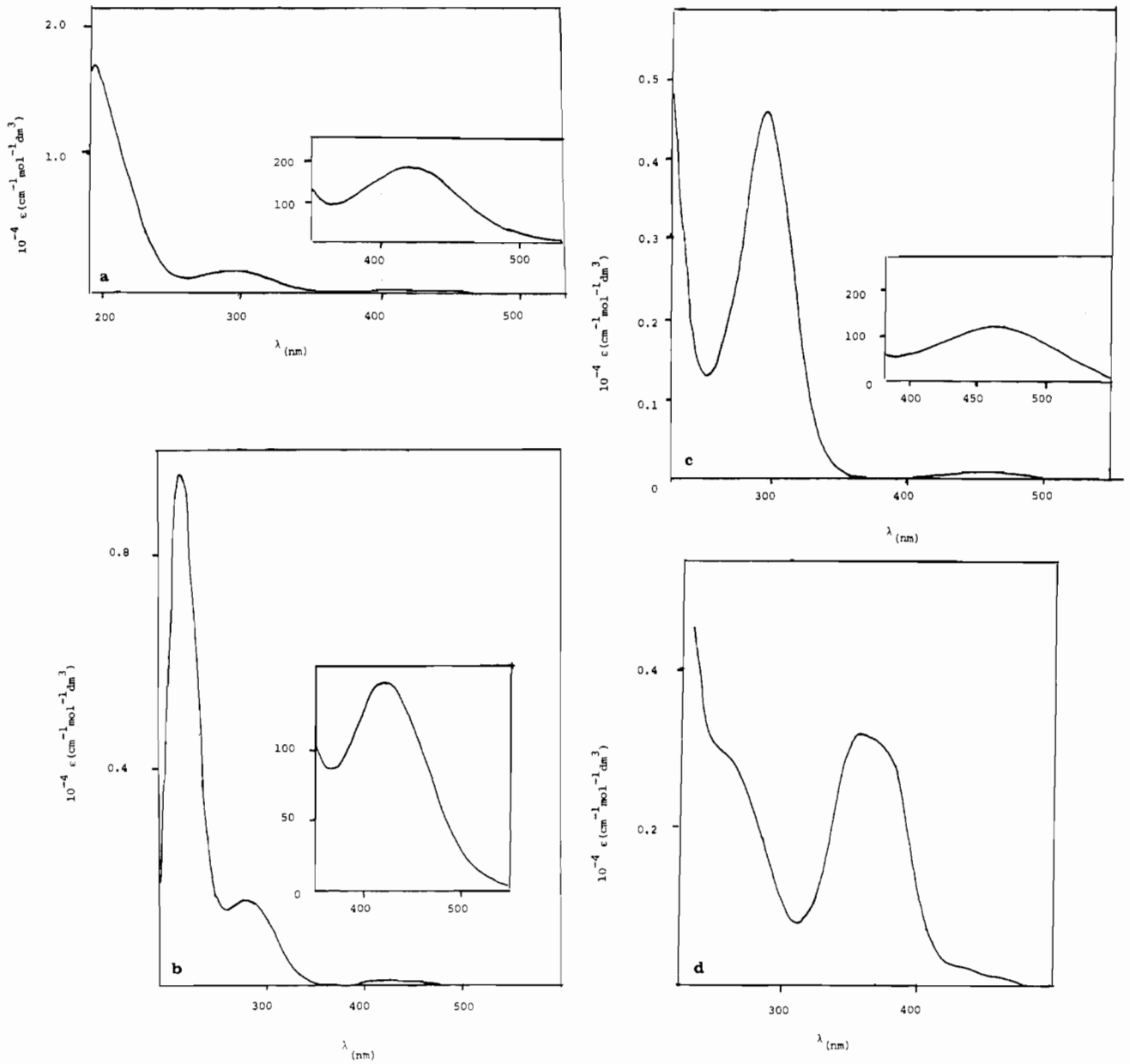

Figure 9. UV–vis spectra in CH_3CN: (a) *trans*-$[Ru^{IV}(14\text{-TMC})O(CH_3CN)]^{2+}$; (b) *trans*-$[Ru^{IV}(14\text{-TMC})O(Cl)]^{+}$; (c) *trans*-$[Ru^{IV}(14\text{-TMC})O(NCO)]^{+}$; (d) *trans*-$[Ru^{IV}(14\text{-TMC})O(N_3)]^{+}$.

Table IX. Comparison of the Reactivity of Different *trans*-Dioxoruthenium(VI) Complexes toward the Catalytic Aerobic Oxidation of Benzyl Alcohol to Benzaldehyde at Room temperature

complex	reacn conditions: quant of complex, mol	reacn conditions: quant of $PhCH_2OH$, mL	reacn conditions: time, h	mol ratio of benzaldehyde to complex
trans-$[Ru^{VI}(14\text{-TMC})O_2][ClO_4]_2$	7.83×10^{-5}	0.5	17	2.5
trans-$[Ru^{VI}(15\text{-TMC})O_2][ClO_4]_2$	8.53×10^{-5}	0.5	18	2.8
trans-$[Ru^{VI}(16\text{-TMC})O_2][ClO_4]_2$	7.60×10^{-5}	0.5	18	2.2
trans-$[Ru^{VI}(TMEA)_2O_2][ClO_4]_2$	7.56×10^{-5}	0.5	18	2.5

Table X. Reactions of *trans*-$[Ru^{IV}(14\text{-TMC})O(CH_3CN)][PF_6]_2$ with Organic Substrates

substrates	reacn conditions: quant of complex, mol	reacn conditions: quant of substrate, mL	reacn conditions: temp, °C	reacn conditions: time, h	reacn conditions: inert atmosphere	products identified (techniques used)	mol ratio of product to complex
benzyl alcohol	6.37×10^{-5}	0.5	28	21		benzaldehyde (GC; GC-MS)	5.4
	1.06×10^{-4}	0.5	25	24	argon	benzaldehyde (GC; GC-MS)	0.9
cyclohexene	1.97×10^{-4}	1	50	18		nil (GC)	

but with different *trans*-dioxoruthenium(VI) complexes. The macrocyclic ring size has little effect on the reactivities of these complexes.

trans-$[Ru^{VI}(14\text{-TMC})O_2][ClO_4]_2$ is inert toward the oxidation of saturated alkanes such as cyclohexane. However, with cyclohexene, oxidation at the allylic carbon occurred with 2-cyclohexen-1-one as the only product. No cyclohexene oxide was detected which indicates the preferential attack of the activated

Table XI. Comparison of the Reactivity of Different Ru(IV)–Monooxo Complexes toward the Catalytic Aerobic Oxidation of Benzyl Alcohol to Benzaldehyde at Room Temperature (28 °C)

complex	reacn conditions: quant of complex, mol	reacn conditions: quant of $C_6H_5CH_2OH$, mL	reacn conditions: time, h	mol ratio of benzaldehyde to complex
trans-$[Ru^{IV}(14\text{-TMC})O(Cl)]ClO_4$	1.15×10^{-4}	0.5	17	3.2
trans-$[Ru^{IV}(14\text{-TMC})O(NCO)]ClO_4$	9.41×10^{-5}	0.5	18	3.9
trans-$[Ru^{IV}(14\text{-TMC})O(N_3)]ClO_4$	8.78×10^{-5}	0.5	21	5.6
trans-$[Ru^{IV}(TMC)O(CH_3CN)][ClO_4]_2$	6.37×10^{-5}	0.5	21	5.4
trans-$[Ru^{IV}(15\text{-TMC})O(Cl)]ClO_4$	9.67×10^{-5}	0.5	21	5.7
trans-$[Ru^{IV}(15\text{-TMC})O(N_3)]ClO_4$	9.39×10^{-5}	0.5	18	3.7
trans-$[Ru^{IV}(15\text{-TMC})O(CH_3CN)][ClO_4]_2$	8.30×10^{-5}	0.5	18	3.8
trans-$[Ru^{IV}(TMEA)_2O(Cl)]ClO_4$	4.41×10^{-5}	0.5	21	5.8

C—H bond over the C= double bond by *trans*-$[Ru^{VI}(14\text{-TMC})O_2][ClO_4]_2$. This observation is in contrast with that found for *trans*-$[Ru^{VI}(TMP)O_2]$, which reacted with cyclohexene giving cyclohexene oxide as the predominant product.[17,27] The differential reactivity between *trans*-$[Ru^{VI}(14\text{-TMC})O_2]^{2+}$ and *trans*-$[Ru^{VI}(TMP)O_2]$ is understandable. In the latter system, a long Ru=O bond is expected, and this favors the oxo transfer reaction. The short and hence strong Ru=O bond in *trans*-$[Ru^{VI}(14\text{-TMC})O_2]^{2+}$ [d(Ru=O) = 1.70–1.71 Å) will favor the hydride/hydrogen atom abstraction. Toluene is also oxidized by *trans*-$[Ru^{VI}(14\text{-TMC})O_2][ClO_4]_2$ although the yield of the products is comparatively low (ca. 5%). The major reaction products were identified as benzaldehyde and benzyl alcohol. No attack on the aromatic ring was found.

The Ru^{IV}=O tertiary amine complexes are weaker oxidants than their parent Ru(VI)–dioxo species. No reaction was observed between $[Ru^{IV}(L)O(X)]^{n+}$ with olefin and cyclohexene, but they did oxidize benzyl alcohol to benzaldehyde (Tables X and XI). The reaction stoichiometry of *trans*-$[Ru^{IV}(L)O(X)]^{n+}$ to benzaldehyde is ca. 1:1 under argon atmosphere, in accordance with an overall two-electron process

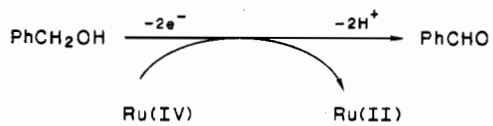

In the presence of air, *trans*-$[Ru^{IV}(L)O(X)]^{n+}$ also catalyzed the aerobic oxidation of benzyl alcohol. All Ru^{IV}=O complexes exhibited similar catalytic oxidative behavior (Table X).

The relative inertness of the Ru(IV)–oxo complexes of tertiary amine toward organic substrate oxidation is in sharp contrast to the reported works on $[Ru^{IV}(trpy)(bpy)O]^{2+}$ and related complexes.[18,26] The Ru^{IV}=O complexes containing π-aromatic amine ligands are active oxidants, capable of undergoing hydride abstraction and epoxidation under mild conditions.[3d,26] The differential reactivity between *trans*-$[Ru^{IV}(14\text{-TMC})O(CH_3CN)]^{2+}$ and $[Ru^{IV}(trpy)(bpy)O]^{2+}$ is understandable, since the latter system is more oxidizing and has a weaker Ru=O bond.

Conclusion

We have demonstrated here that stable Ru=O complexes could be obtained with the central metal ion in the IV, V, and VI oxidation states. As expected, trans Ru(VI)–dioxo complexes are stronger oxidants than the corresponding Ru^{IV}=O species. In general, the Ru(IV) system possesses weaker metal–oxo bond than the Ru(VI) system, indicating that they are in general better candidates for oxo transfer reactions. Axial ligation does not perturb the Ru=O bond in the Ru(IV) state, but the oxidation potential and reactivity of *trans*-$[Ru^{V}(L)O(X)]^{n+}$ system vary with the nature of the coordinated axial ligands. Replacement of the σ-saturated amine by the π-aromatic one increases both the metal–oxo bond length and the oxidation potential of the Ru=O complexes. It would therefore be expected that high-valent ruthenium oxo complexes containing π-aromatic amines will show promising oxidation chemistry as suggested by Meyer and coworkers.[3]

Acknowledgment. C.-M.C. and K.-Y.W. acknowledge financial support from the Committee of Conference and Research Grants of University of Hong Kong. Helpful discussions with H. B. Gray and V. M. Miskowski on certain aspects of electronic spectroscopy are also acknowledged. We also thank T. C. W. Mak for his help in part of the X-ray structure work. T.-F.L. acknowledges support from the National Institute of General Medical Sciences, USPHS, Grant No. GM-16966 (R. E. Marsh), during her leave at the California Institute of Technology.

Registry No. *trans*-$[Ru(14\text{-TMC})O_2](PF_6)_2$, 95978-19-1; *trans*-$[Ru(15\text{-TMC})O_2](ClO_4)_2$, 98938-47-7; *trans*-$[Ru(16\text{-TMC})O_2](ClO_4)_2$, 98938-50-2; *trans*-$[Ru(TMEA)_2O_2](ClO_4)_2$, 98938-52-4; *trans*-$[Ru(14\text{-TMC})O_2]ClO_4$, 103056-18-4; *trans*-$[Ru(14\text{-TMC})O(CH_3CN)](PF_6)_2$, 98767-23-8; *trans*-$[Ru(14\text{-TMC})O(Cl)]ClO_4$, 98938-54-6; *trans*-$[Ru(14\text{-TMC})O(N_3)]ClO_4$, 108452-21-7; *trans*-$[Ru(14\text{-TMC})O(NCO)]ClO_4$, 108452-22-8; *trans*-$[Ru(15\text{-TMC})O(CH_3CN)](ClO_4)_2$, 108452-24-0; *trans*-$[Ru(15\text{-TMC})O(Cl)]ClO_4$, 99350-79-5; *trans*-$[Ru(15\text{-TMC})O(N_3)]ClO_4$, 108452-26-2; *trans*-$[Ru(TMEA)_2O(Cl)]ClO_4$, 108452-28-4; *trans*-$[Ru(14\text{-TMC})O_2](ClO_4)_2$, 95978-18-0; *trans*-$[Ru(15\text{-TMC})O_2]^+$, 108452-29-5; *trans*-$[Ru(16\text{-TMC})O_2]^+$, 108452-30-8; *trans*-$[Ru(TMEA)_2O_2]^+$, 108452-31-9; *trans*-$[Ru(14\text{-TMC})O(CH_3CN)](ClO_4)_2$, 108452-32-0; *trans*-$[Ru(14\text{-TMC})Cl_2]ClO_4$, 95785-32-3; *trans*-$[Ru(15\text{-TMC})O(OH_2)]^{2+}$, 108452-33-1; *trans*-$[Ru(16\text{-TMC})O(OH_2)]^{2+}$, 108452-34-2; *trans*-$[Ru(TMEA)_2O(OH_2)]^{2+}$, 108452-35-3; *trans*-$[Ru(15\text{-TMC})(OH)(OH_2)]^{2+}$, 108452-36-4; *trans*-$[Ru(16\text{-TMC})(OH)(OH_2)]^{2+}$, 108452-37-5; *trans*-$[Ru(TMEA)_2(OH)(OH_2)]^{2+}$, 108452-38-6; *trans*-$[Ru(14\text{-TMC})O(Cl)]^{2+}$, 98938-55-7; *trans*-$[Ru(15\text{-TMC})O(Cl)]^{2+}$, 98938-56-8; *trans*-$[Ru(TMEA)_2O(Cl)]^{2+}$, 108452-39-7; *trans*-$[Ru(14\text{-TMC})O(NCO)]^{2+}$, 108452-40-0; *trans*-$[Ru(14\text{-TMC})O(N_3)]^{2+}$, 108452-41-1; *trans*-$[Ru(15\text{-TMC})O(N_3)]^{2+}$, 108452-42-2; *trans*-$[Ru(15\text{-TMC})Cl_2]Cl$, 101981-47-9; *trans*-$[Ru(TMEA)_2Cl_2]Cl$, 108452-43-3; *trans*-$[Ru(16\text{-TMC})Cl_2]Cl$, 101981-49-1; *trans*-$[Ru(14\text{-TMC})Cl_2]Cl$, 92141-42-9; PPh_3, 603-35-0; benzyl alcohol, 100-51-6; 2-propanol, 67-63-0; benzaldehyde, 100-52-7; cyclohexene, 110-83-8; cyclohexane, 110-82-7; toluene, 108-88-3; hydrogen peroxide, 7722-84-1.

Supplementary Material Available: Tables of molar conductivity (Table S1) and magnetic susceptibility (Table S2) measurements and anisotropic temperature factors (3 pages); a table of calculated and observed structure factors (6 pages). Ordering information is given on any current masthead page.

(27) Che, C. M., unpublished work.